Transactions on Networks and Communications - Vol. 9, No. 3
Publication Date: June, 25, 2021
DOI: 10.14738/tnc.93.10214.
Neelakanta, P., & Groff, D. D. (2021). Conceiving Inferential Prototypes of MIMO Channel Models *via* Buckingham's Similitude Principle for 30+ GHz through THz Spectrum. Transactions on Networks and Communicaitons, 9(3). 1-35.

Conceiving Inferential Prototypes of MIMO Channel Models *via* Buckingham's Similitude Principle for 30+ GHz through THz Spectrum

Perambur Neelakanta
Department of Computer and Electrical Engineering and Computer Science
Florida Atlantic University, Boca Raton, FL 33431, United States

Dolores De Groff
Department of Computer and Electrical Engineering and Computer Science
Florida Atlantic University, Boca Raton, FL 33431, United States

ABSTRACT

Facilitating newer bands of 'unused' segments (windows) of RF spectrum falling in the mm-wave range (above 30+ GHz) and seeking usable stretches across unallocated THz spectrum, could viably be considered for Multiple Input Multiple Output (MIMO) communications. This could accommodate the growing needs of multigigabit 3G/4G applications in outdoor-based backhauls in picocellular networks and in indoor-specific multimedia networking. However, in contrast with cellular and Wi-Fi, wireless systems supporting sub-mm wavelength transreceive communications in the outdoor electromagnetic (EM) ambient could face "drastically different propagation geometry"; also, in indoor contexts, envisaging pertinent spatial-multiplexing with directional, MIMO links could pose grossly diverse propagation geometry across a number of multipaths; as such, channel-models based on stochastic features of diverse MIMO-specific links in the desired test spectrum of mm-wave/THz band are sparsely known and almost non-existent. To alleviate this niche, a method is proposed here to infer sub-mm band MIMO channel-models (termed as "prototypes") by judiciously sharing "similarity" of details available already pertinent to traditional "models" of lower-side EM spectrum, (namely, VLF through micro-/mm-wave). Relevant method proposed here relies on the "principle of similitude" due to Edgar Buckingham. Exemplar set of "model-to-(inferential)-prototype" transformations are derived and prescribed for an exhaustive set of fading channel models as well as, towards estimating path-loss of various channel statistics in the high-end test spectrum.

Keywords: Channel/propagation-models, mm-wave/THz spectrum, Similitude principle, Wireless communication

INTRODUCTION

With alarming increase in radio-frequency (RF) spectrum utilization and almost fully occupied status of available electromagnetic (EM) spectral windows, facilitating newer ranges of RF-spectrum for wireless communication is an explicit necessity, so as to accommodate the growing needs of broad-bandwidth wireless applications. For example, enabling newer ranges of 'unused' segments (windows) of RF spectrum in the mm-wave band (above 30+ GHz) and

seeking usable stretches across the unallocated THz spectral range could possibly considered for Multiple Input Multiple Output (MIMO) communications in accommodating the growing needs of multigigabit 3G/4G applications enclaving outdoor-based backhauls in picocellular networks and indoor-specific multimedia networking. However, in contrast with those of cellular and Wi-Fi systems, usage of smaller, carrier wavelengths (of mm-wave/THz bands) in outdoor EM ambient could pose "drastically different propagation geometry"; and, in indoor contexts, pertinent directional mm/THz wave propagations across spatially-multiplexed, line-of-sight (LoS) MIMO links may also face grossly diverse propagation geometry with multiple number of paths plus nodes of relatively small form-factors. Further, moderately separated antennas facilitating such directional links, could lead to sparse EM scattering; but, increased propagation loss in the transreceive paths is inevitable with smaller wavelengths [1] [2].

MIMO techniques, in general, are adopted to combat fading; and, suppose carrier frequencies falling in the mm/THz wave bands are prescribed for such MIMO systems in order to achieve multigigabit 3G/4G applications in outdoor-based backhauls (of picocellular networks) and in indoor-specific multimedia networking. The associated EM propagation artifacts and interference characteristics of such MIMO-links would pose unique stochastic features and distinct propagation characteristics thanks to (small) carrier wavelength *versus* spacing between the antenna elements and limited EM-scattering involved. Such details could render the elements of the MIMO-channel matrix not always being independent.

Use of mm/THz wave spectrum hardly prevails in the state-of-the-art communication areas (including MIMO systems); as such, relevant neoteric paradigms of spectrum utilization consist of only a limited/sparse and/or mostly insufficient data detailing the underlying EM wave propagation characteristics. Thus, a lacuna prevails in the comprehension of channel-models at this spectral range of interest. As such, this study is motivated to address the sparsity of MIMO channel modeling *vis-à-vis* fading and path-loss features; and, the scope of this paper is set to explore the feasibility of conceiving relevant "inferential prototypes" of channel-models in the said EM spectral range (for possible adoption in MIMO contexts). The proposed method is based on judiciously sharing the "similarity" of details between already existing (known) "models" of traditional, lower-side EM spectrum, (namely, VLF through micro-/mm-wave) availed as *ex post* data and the corresponding "prototypes" are conceived as *ex ante* details inferred for the test-bands (of mm-wave through THz spectrum). Relevant method relies on the so-called "principle of similitude" due to Edgar Buckingham [3]. Illustrative "model-to-(inferential)-prototype" transformations are derived and discussed with reference to an exhaustive set of channel-models on fading and path-loss characteristics pertinent to diverse channel statistics.

Commensurate with the objectives indicated above, this paper is organized as follows: The next section (Section 2) reviews the general aspects of wireless channel-models and summarizes the specific aspects of MIMO-channels. Further, focused considerations on such channel characterizations in the 30+ GHz through THz spectrum are outlined and associated concerns are identified. In Section 3, the proposed heuristics of inferring "prototypes" of EM propagation characteristics required at the high-end spectral range (of mm-wave/THz band) using the prior known (available) "models" at lower bands (like UHF/microwaves) is described. Relevant systematic procedure in judiciously projecting the associated "similarity" of details in the "models" (of low-frequency end) into "inferential prototypes" of high-end RF-channels (representing the test-bands of interest) is described in Section 4 in terms of the heuristics of

the so-called *principle of similitude* (advocated by Edgar Buckingham [3]). The similitude considerations involved in the model-to-(inferential) prototype transformations are elaborated in Section 5 and applied to illustrate fading statistics and path-loss characteristics of channel-models at the test frequency bands of interest, (namely, 30+ GHz through THz EM spectrum). Section 6 lists the well-known "models" of fading channels with the associated parameters; hence, the corresponding deduced "inferential prototypes" are presented with descriptive notes on an exhaustive set of fading statistics. Similarly, "model-to-(inferential)-prototype" transformations are illustrated to deduce path-loss characteristics the channels in the test bands of interest. Discussions on the proposed methods are furnished in Section 7 and pertinent remarks are given in the closure section (Section 8).

WIRELESS- AND MIMO-CHANNEL MODELS: AN OVERVIEW

Modeling wireless communication ambient describing the associated RF propagation and channel characteristics has been the topic of interest with the advent of mobile communications and extensive proliferation of cellular networks. Relevant details enclaving transmissions at traditional HF through UHF/microwave frequencies are addressed exhaustively in the literature [4-8]. Associated channel-models reflect the propagation characteristics of signals in pertinent radio environments are essentially needed for evaluating the performances of wireless communication systems. Typically, commencing from the simple free-space model, channel characteristics of both outdoor and indoor contexts are indicated for traditional wireless systems in a gamut of published efforts. To name a few, are the so-called: Lee's model, Langley-Rice model, Okumura model, Hata model, Walfish and Bertoni model, Hashemi model, Rappaport's SIRCIM model, Saleh and Valenzula model and Seidal and Rappaport model [4-8].

In wireless systems, the EM propagation ambient supporting communication links decides the integrity of transreceive signals largely specified by the underlying fading and path-loss characteristics. Fading implies variations (with stochastic attributes) seen in the signal attenuation *versus* time, locales of transreceive units and carrier frequency. That is, fading denotes a random process caused by probabilistic variates on EM propagation due to multipath and/or shadowing effects from the obstacles. Path-loss is another channel artifact denoting the EM energy losses encountered in wireless communications that incur on terrestrial paths through atmospheric environment as well as, in the content-infested indoor ambient.

In all, due to fading and path-loss characteristics, the transmitted wireless signal across its transceive path would invariably seen morphed at the receiving end. Relevant profile of such received signals can then be specified in terms of the details on the transmitted signal (known *a priori*), if a model for the medium/channel between the transceive entities is also available. Such characterization of RF signal transit-paths is well-known as a "channel-model"; and, it in essence, represents the EM propagation profile of the signal and the associated statistics of signal-strength fluctuations across the channel in question; and, a number of channel-models have been evolved as listed earlier. The *pros* and *cons* of channel considerations in realizing practical RF communication links are fairly comprehended in the traditional wireless systems pertinent to classical deployment of VLF through microwave frequencies.

The perspectives of channel-models become even more unique and visibly complex in the contexts of multiple-input multiple-output (MIMO) technique ushered into wireless communications in order to achieve a significant increase in data throughput as well as, link

reliability (mostly without extra bandwidth or boosting transmission power) [9-11]. MIMO together with orthogonal frequency division multiplexing (OFDM) has proliferated as a key technique in the long-term evolution (LTE) of 3G/4G cellular networks. In its conception to achieve higher throughputs within a given bandwidth *via* space diversity schemes, the MIMO-links were typically modeled in the early theoretical studies (due to Telatar [12] and Foschini [13]) as narrowband random MIMO channels. Such efforts refer to evolving a simple channel-model represented by a matrix [**H]** with M-transmit and N-receive antennas.

In the expanded applications, MIMO channel models have been subsequently framed for different EM environments; and, comparison between channel-models is done on the basis of the associated theoretical considerations *versus* measured data. Relevantly, two kinds of channel models, namely, correlation-based stochastic models (CBSMs) and geometry-based stochastic models (GBSMs), are prescribed (commensurate with IEEE 802.11n standards) in order to evaluate the performances of the wireless communication systems; and, the former being less complex is typically used in theoretical evaluations of MIMO system performance. However, the accuracy of CBSM is limited for wireless channels exhibiting non-stationary phenomenon and spherical wave effects. In contrast, GBSM is considered as being accurate in portraying the realistic channel properties of massive MIMO channel applications (in spite of the associated higher computation complexity).

MIMO techniques in general are indicated for combating fading. The underlying channel characterizations, however are unique and mostly differ from those of non-MIMO strategies, even at lower carrier frequencies. As such, exclusive MIMO-channel models have been developed. Typically, the MIMO channel characterization is exemplified *via* a lamp-post based outdoor deployment model (for example, as in a mesh backhaul), which duly accounts for fading due to ground and wall reflections; and, in indoor contexts, the MIMO infrastructure with space diversity and spatial multiplexing (for example, as done in "streaming high-definition television from a set-top box to a television set"), relevant (MIMO)-channel model becomes even more unique with a number of eigen modes framing the form-factor of the channel involved [1].

The MIMO-specific channel-models have been comprehensively studied at traditional lower end of EM spectrum [9-11]. Though restrictedly addressed (on *ad hoc* basis), pertinent channel considerations and channel-modeling in the millimeter wave regime of RF systems [14] including the MIMO-links [1] also exist. Yet, such a comprehension is rather sparse and even absent for the EM spectrum ranging 30+ GHz through THz. However, such details are highly desirable and imminent in any aggressive suite of implementing the current needs of robust wireless communication links including MIMO systems. Specifically, MIMO channel-modeling in the high-end spectral range of 30+ GHz through THz is needed towards profitable use of the large extents of bandwidth available in the said test bands of interest. Pertinent uses as stated before refer to realizing multi-Gigabit wireless networks with applications ranging from indoor multimedia networking to accommodating outdoor backhauls for picocellular networks. However, using the spectral range of 30+ GHz through THz in such applications, the carrier wavelengths involved are obviously an order (or orders) of magnitude smaller than those in the existing cellular and Wi-Fi systems. As such, significantly different propagation geometry can be foreseen in the underlying EM ambient. For example, omnidirectional transmission is almost ruled out because of the increased propagation losses encountered at smaller

wavelengths. So, highly directive transreceive MIMO-links can be envisaged with electronically steerable beams formed by compact antenna arrays. As a result, only a small number of paths would dominantly prevail (in such directional small-wavelength links), posing a sparse scattering ambient unlike, the rich scattering environment at lower carrier frequency operations. Usage of small wavelengths also implies achieving spatial-multiplexing gains even in LoS transreceive links or more generally, in the ambient of sparse scattering consistent with the dispersed of antennas having moderate separations.

As stated earlier, knowledge on EM propagation characteristics (or channel models) in the said mm/THz bands (henceforth addressed as the "test-bands") is still primitive and mostly unknown for applications in MIMO-systems or otherwise. Filling this niche will conform to transformational improvements in using the radio spectrum of test-bands containing 'unused' segments (windows) in mm-band (above 30+ GHz) and usable stretches across the unallocated THz frequencies. Hence, it will add a dimension of realism in conceiving the exploding broadband communication needs (including novel MIMO applications), so as to support the associated traffic intensity of triple-play wireless communication services in the near-future and beyond.

Hence proposed in this paper is a feasibility consideration on a very practical problem: How can channel/propagation models be inferentially deduced for the spectral range of test-bands from the existing (available) knowledge on the lower strata of EM spectrum? And the solution sought thereof, is to find one-to-one correspondence between the channel characteristics (dubbed as "models") known *ex post* at low-frequencies and corresponding 'scaled-up' channel features (called "prototypes") attributed *ex ante*, to higher (test) frequencies of interest.

INFERRING "PROTOTYPES" FROM "MODELS": PROPOSED METHOD AND APPROACH

As indicated above, the present study objectively proposes an approach to develop "prototypes" of EM propagation and channel characterizations of RF signal transmissions in the test frequency bands covering the new frontiers of (almost) unused 30+ GHz spectral windows and mostly unexplored terahertz span (above 275 GHz *sans* spectrum allocations). As briefed above, relevant concept is illustrated in Figure 1.

The proposed approach towards developing "prototypes" of EM propagation and related channel characterizations of RF signal transmissions in the spectral bands of (almost) unused 30+ GHz frequencies indicated above (and illustrated in Figure 1) is summarized as follows:

- A set of channel details are presumably known *a priori* at lower frequency bands (like UHF/microwaves). The set of such *ex post* features are designated as the "model"
- The said "model" details are listed and judiciously projected to frame a "inferential prototype" at the desired high-end frequency (test-band); and, the *ex ante* set of features so conceived denote an inferred "prototype" that shares the "similarity" of all the pertinent details in the "model"
- The projection of shared similarity indicated above is done *via* a systematic procedure based on the so-called *principle of similitude* advocated by Edgar Buckingham [3] in terms of dimensional analyses perspectives detailed in the next section.

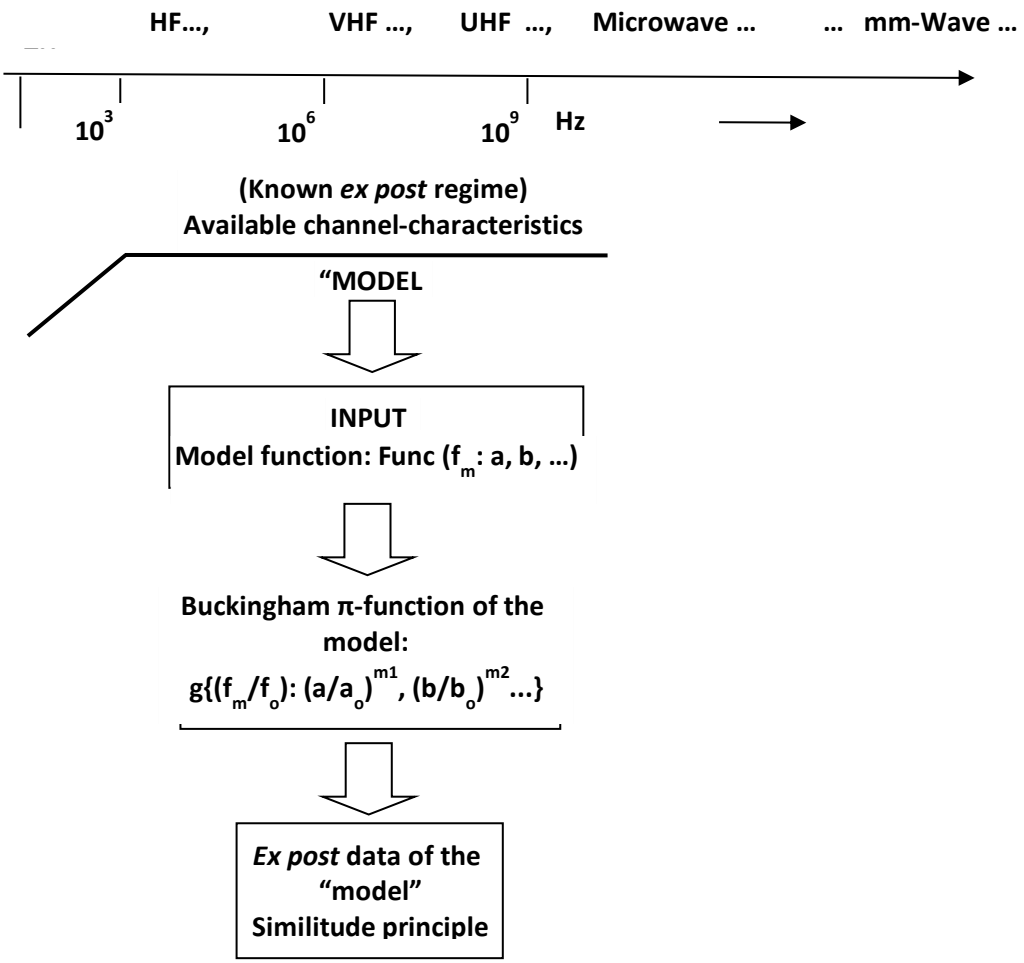

Figure 1. Specifying a "model" function denoting a set {a, b, ...} of known data on channel attributes at lower-end frequency spectrum (f_m) towards formulating a corresponding π-function (for use to infer the "prototype" function as indicated in Step 2). The set {a_o, b_o…,} denotes reference entities that render the variable set {a, b, …,} dimensionless; and, {(m1, m2, …)} are pertinent exponents prescribed to frame the π-relations consistent with Buckingham's similitude principle.

The steps in conceiving "inferential prototypes" of RF channel characteristics in a desired test-band using the "model" data available at lower frequencies are as follows:

- Step 1: Construction of the "model": This is illustrated in Figure 1. The channel parameters {a, b, …} known *a priori* at lower frequencies, f_m (say, HF through microwaves) are first identified and specified as the "model" features denoted by a functional relation: Func(f_m: a, b,…). This model function is then modified and rewritten, following the so-called as *Buckingham's similitude principle* described in the next section. Relevantly, a Buckingham π-function of the model is specified as: g[(f_m/f_o): $(a/a_o)^{m1}$, $(b/b_o)^{m2}$...], where f_o is a reference frequency prescribed to normalize, f_m; and, {a_o, b_o, ...} etc. are normalizing parameters indicated respectively, for the elements of the set {a, b,…}; and, the set {m1, m2, ...} depicts appropriate exponents indicated for the aforesaid π-relation. This "model" prescription as above depicts *ex post* details of the channel in question.

- Step 2: Inferring the "prototype" details refer to *ex ante* deductions: The "prototype" can be obtained by using *ex post* details of the "model" (of Step 1) as illustrated in Figure 2.

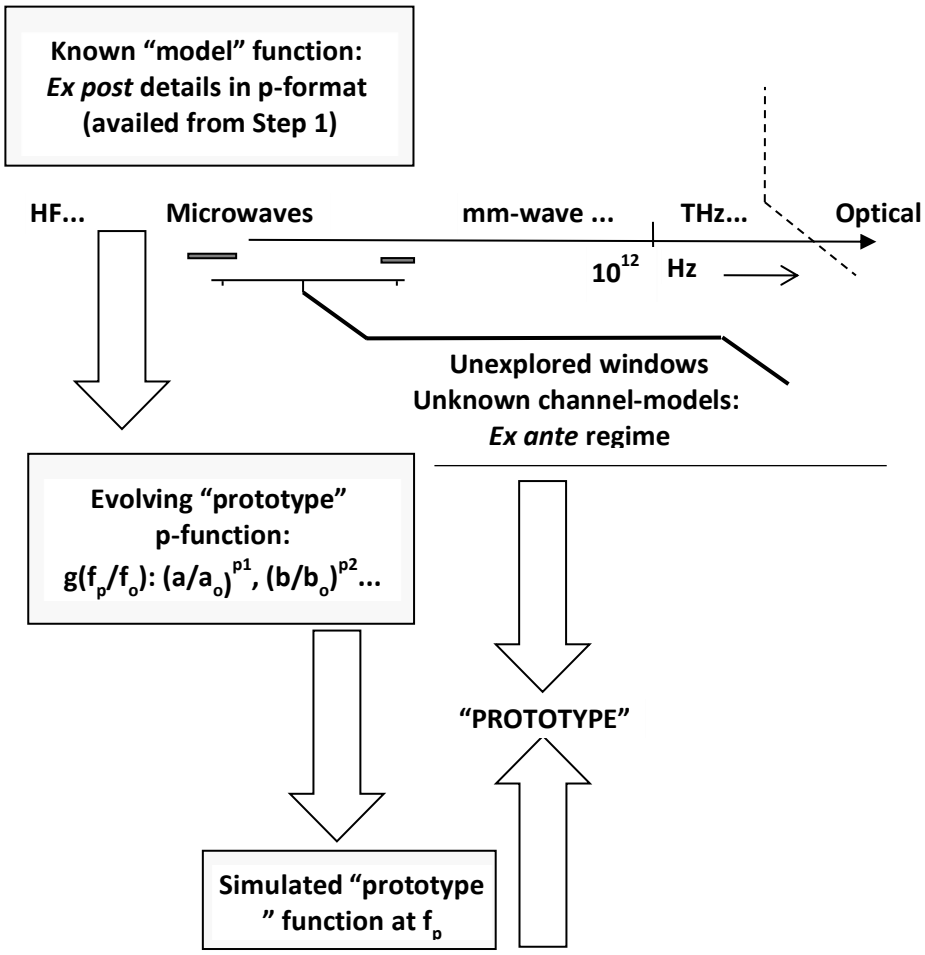

Figure 2. Inferring the "prototype" function $g[(f_p/f_o)$: $(a/a_o)^{p1}$, $(b/b_o)^{p2}$...] of channel characteristics in the higher RF spectra, f_p of the desired test-bands using the known "model" function of *ex post* details (deduced in π-format in Step1 at lower frequency spectra, f_m). (The set $\{a_o, b_o...,\}$ as before denotes reference entities that render the variable set {a, b, ...,} dimensionless; and, {(m1, m2, ...) and, (p1, p2, ...)} are exponents on π-relations). The deduced "prototype" details refer to *ex ante* deductions.

Given the known channel parameters {a, b,…} considered in Step 1 corresponding to lower frequencies, f_m depicting the "model" features and relevantly specified π-form of the Buckingham function, $g\{(f_m/f_o)$: $(a/a_o)^{m1}$, $(b/b_o)^{m2}$...}, the required "prototype" function: $g[(f_p/f_o)$: $(a/a_o)^{p1}$, $(b/b_o)^{p2}$...] can be inferred *via* pertinent transformation of: $g\{(f_m/f_o)$: $(a/a_o)^{m1}$, $(b/b_o)^{m2}$...} $\Leftrightarrow$ $g[(f_p/f_o)$: $(a/a_o)^{p1}$, $(b/b_o)^{p2}$...] as explained in the next section. The inferred "prototype" denotes *ex ante* profile of channel characteristics sought in the higher RF spectra, f_p of the desired test-bands. Again, in $g[(f_p/f_o)$: $(a/a_o)^{p1}$, $(b/b_o)^{p2}$...], the set $\{a_o, b_o...,\}$ denotes reference entities that render the variable set {a, b, …,} dimensionless; and, {(m1, m2, …) and,

(p1, p2, …)} are appropriate exponents imposed on π-relations consistent with Buckingham's similitude principle (as will be explained in the pursuant section).

BUCKINGHAM'S SIMILITUDE PRINCIPLE

The similitude principle has been deployed extensively in various disciplines, to name a few: Model-based testing and evaluations of structures in civil, aeronautical/aerospace, naval architecture [15], reliability predictions [16], radar cross-section (RCS) studies [17] etc. The underlying considerations of similitude concept can be outlined as follows:

- Evolving a "prototype" refers to elucidating a set of new descriptive details formulated *a posteriori* and prescribed on an entity (for example, a structure or a phenomenon). Such inferred (*ex ante*) details correspond to an existing and available set of *ex post* data (referred to as the "model"). Such data is presumably known *a priori* on the entity in question. The underlying one-to-one transformation is inferred and interpreted *via* similitude considerations based on the *theory of modeling* consistent with the norms of dimensional analysis
- The underlying theoretics and mathematical description of *theory of dimensions* (evolved in terms of dimensions and units) is aptly applied to portray the similitude aspects of the prior knowledge on the said "model" (depicting the physical entity or phenomenology) *versus* the "prototype" posterior information being sought, subject to the following norms:
  - The mathematical description (of transforming a "model" into a "prototype") should comply with the laws of nature and specified in a dimensionally homogeneous form. That is, regardless of the choice of dimensional units (in which the associated physical variables are measured), the governing equation must be valid
  - All relevant governing equations must be dimensionally homogeneous. That is , an arbitrary equation of the form, $[\text{func}(x_1, x_2, \ldots, x_n) = 0]$ can be alternatively expressed as, $[g(\pi_1, \pi_2, \ldots \pi_m) = 0]$, where the π-terms denote dimensionless products of n physical variables of the set $\{x_1, x_2, \ldots, x_n\}$; and, m = (n – r) with r depicting the number of fundamental dimensions that are involved in the physical variables.

    Explicitly, the second consideration above namely, $[\text{func}(x_1, x_2, \ldots, x_n) = 0] \Leftrightarrow [g(\pi_1, \pi_2, \ldots \pi_m) = 0]$ implies the following: (i) The π-form of physical occurrence can be deduced *via* proper use of dimensions of the n physical quantities, $\{x_i\}_{i = 1, 2, \ldots, n}$ by resorting to dimensional analysis. (ii) In physical systems that differ only in magnitudes of the units (used to measure the n quantities, namely $\{x_i\}_{i = 1, 2, \ldots, n}$), the "model" entity and its reduced or enhanced scale-version ("prototype") will have identical functional, g(.); and, (iii) similitude requirements for modeling result from forcing the π-terms, $\{\pi_i\}_{i = 1, 2, \ldots, m}$ to be equal in the "model" as well as in the "prototype". (This is a necessary condition for the full functional relationships to be equal).

In short, a "model" denotes a representation of the physical system with details (known *ex post*) that can be adopted to infer the behavior of a corresponding "prototype" in some respect. That is, the principle of similitude (due to Buckingham [3]) enables predicting the performance of a

new design (called "a prototype") based on mimicking the data from an existing, similar design (designated as "the model").

In such representations, the first consideration is to show that the two systems can be described in terms of dimensionless numbers as per Buckingham's heuristics. This can be outlined as follows: Given any element (ϕ_m) of the π-set of the model and the corresponding element (ϕ_p) of the prototype, ideally the similarity principle demands, $\phi_p/\phi_m = 1$. But, in practice, at least some first or second-order deviations may be encountered rendering exact model-to-prototype extrapolation, somewhat "distorted" [18]. Conceiving an approximated version *via* piecewise linearization in similarity relations is, however, feasible as will be indicated later in this paper.

In general, the similitude problems based on Buckingham's heuristics can be classified as follows: (i) *Geometric similitude*, which denotes the "model" in question representing an "exact" scale-copy of the "prototype" consistent with physical geometry involved; (ii) *kinematic similitude* concerned with flow considerations, where the "model" flow is set proportional to the corresponding flow in the prototype, preserving the associated vector nature of the flowing entity; and, (iii) *dynamic similitude*, which refers to forces associated in the "model" being proportional to the forces seen in the "prototype". (This is a necessary condition, but not sufficient for dynamic similitude) [11] [19-23].

Relevant to the present study of applying Buckingham's similitude principle in the contexts of channel modeling, first the underlying similitude considerations pertinent to EM theory should be identified. That is, the associated set of postulations and constitutive relations consistent with the linearity aspects of Maxwell's equations [24] should be specified in dimensionless forms by invoking Buckingham's π-theorem. Then, the EM propagation/channel-modeling is rendered viable for the similitude approach. Existing studies on applying such similitude principle in electrodynamics and EM contexts are as follows: (i) Geometrical inferences (relative to wavelength) such as in antenna designs [25], radar cross-section (RCS) evaluations [17]; (ii) channel characterizations [26] (studied in a limited extent) and (iii) frequency-scaling of rain attenuation (such as in ITU-R Rec.P.618-7, 2001 and similar models [27] [28]).

Basically, the kinematic/dynamic similitude is applied in EM contexts considering (i) the flow of electric current signified by the time-varying states or dynamics of electric charges, (ii) the rate of change of electric/magnetic flux and (iii) the Poynting vector flow. EM similitude technique has also been advocated in studying laser scattering [23]. Typically, electrodynamic similitude is applied to model the nondispersive targets as indicated in [22].

Applying π-theorem in EM contexts

In all, the heuristics of adopting Buckingham's π-theorem in the contexts of electromagnetism (EM) and hence, applying the principle to elucidate the "prototypes" of channel-models *vis-à-vis* EM propagation characteristics in wireless communications involve the following basics of EM theory outlined to deduce the associated π-relations.

As well known, the EM waves possess a characteristic wavelength length (λ in m), which is related to their frequency (f in Hz) by the relation, λ (m) = [v in m/s)/f in Hz] where, v denotes the velocity of propagation of EM wave in the medium of interest and f is the frequency of the

EM wave. For free-space propagation, $v \equiv c$ (= 3×10^8 m/s) as decided by the associated constants of the free-space, namely, the absolute permittivity $\varepsilon_o = (1/36\pi) \times 10^{-9}$ farad/meter and absolute permeability, $\mu_o = (4\pi) \times 10^{-7}$ henry/meter; and, $c = 1/(\mu_o\varepsilon_o)^{1/2}$ m/s, (= 3×10^8 m/s depicting the speed of the light). And, $v = c/(\mu_r\varepsilon_r)^{1/2}$ m/s [24] expressed in terms of (dimensionless) relative permittivity and permeability, (ε_r, μ_r) of the medium; hence, for free-space, ($\varepsilon_r = 1$; $\mu_r = 1$).

An example of elucidating dimensionless parameters, functions, equations etc. in the contexts of electrodynamics as required in similitude applications is as follows: Considering the well-known Coulomb's law of force ($|\mathbf{F}|$) between given two charges of q_1 and q_2 units, separated by a distance d units in a dielectric medium characterized by a (dimensioned) constant, k, the said law is specified by the equation, $\{\text{func}(x_1, x_2, \ldots, x_n) = 0\} \Rightarrow \text{func}[|\mathbf{F}|, k, (q_1, q_2), d] = 0$; explicitly, this Coulomb's law can be written as: $\{[|\mathbf{F}| - k\, q_1q_2/d^2]\} = 0$. In terms of the associated units term-by-term, Coulomb's law can be rewritten as: func{[K_1 force unit] − [K_2 (capacitance unit/length unit)$^{-1}$ × K_3 (charge unit)^2]/[K_4(length unit)^2] = 0}, where, the func{.} is expressed in terms of corresponding fundamental measures that describe the associated quantities; and K_1, K_2 and K_3 are relevant proportionality constants.

The above relation holds for any system of units, (CGS, SI or FPS) for force, capacitance, charge and length; and as such, it is dimensionally homogeneous. Now, in terms of the notions of Buckingham [3], the implicit functional relation of Coulomb's law, namely, $\text{func}[|\mathbf{F}|, k, (q_1, q_2), d] = 0$ can also be represented as a product of powers in a form as follows: $|\mathbf{F}| = C_D \times [k^{\gamma}(q_1, q_2)^{\alpha}d^{\beta}]$ newton, where C_D is a dimensionless parameter, (which by itself could be a function of dimensionless groupings of some pertinent physical entities; or, it can be a simple constant, otherwise); and, the exponents $\gamma = +1$, $\beta = -2$ and $\alpha = +2$ are explicitly pertinent to the Coulomb's law under discussion.

Next, the functional relation, $F = C_D[k^{\gamma}(q_1, q_2)^{\alpha}d^{\beta}]$ can be cast in the π-form, $\{g(\pi_1, \pi_2, \ldots, \pi_m) = 0\}$ using similitude principle. Relevantly, consistent with Buckingham's π-theorem, the dimensionally homogeneous equation, $\{\text{func}[|\mathbf{F}|, k, (q_1, q_2), d] = 0\}_{n=4}$ is reduced to an equivalent equation involving a set of dimensionless products, namely, $\{g(\pi_1, \pi_2, \ldots, \pi_m) = 0\}_{m=2} \equiv \{g(kq^2/Fd^2, q^2F/kd^2) = 0\}$. In other words, the given equation, $\{\text{func}(x_1, x_2, \ldots, x_n) = 0\} \Rightarrow \{\text{func}[F, k, (q_1, q_2), d] = 0\}_{n=4}$ implies the same Coulomb's law specified in a dimensionless format as: $\{g(\pi_1, \pi_2, \ldots, \pi_m) = 0\} \Rightarrow \{g(kq^2/Fd^2, q^2F/kd^2) = 0\}_{m=2}$.

Likewise, all the postulations and constitutive relations of EM theory based on the linearity aspects of Maxwell's equations [24] can be specified in dimensionless forms by invoking Buckingham's π-theorem *via* relevant algorithmic suites as indicated above. However, distortions may not be uncommon in such similitude comparisons of EM contexts due to dissimilarities that may prevail in the overall geometry, boundary/initial conditions and/or (nonlinear) material (EM medium) implications. In such cases, still a piecewise linearization can be considered [18] as will be illustrated later.

Similitude considerations on EM propagation channel models

Following the similitude notions narrated above relevant to the contexts of electromagnetics, relevant π-relational details can be developed towards deducing EM propagation profiles and

channel-models of wireless communications (in the test-bands of say, mm-wave through THz spectrum). The underlying procedure involves combining size-scaling (geometry similitude) and frequency-scaling (dynamic similitude) as follows: In applying similitude principle in EM problems, any geometrical entity of interest (say, of length (ℓ) can be specified normalized with respect to the corresponding wavelength (λ_p), in the relevant (geometrical) "dimension" of the "prototype"; and this normalized linear size,(ℓ_p/λ_p) depicts the "scaled" version of the (geometrical) "dimension", (ℓ_m/λ_m) of the "model", where, ℓ_m denotes a(known) linear size of the "model". It is normalized with respect to relevant wavelength (λ_m) to get (ℓ_m/λ_m). Geometrical details of scaled-models can be inferred/predicted at high frequencies (small wavelengths) as "prototypes" of objects (like, an aircraft) using known (geometrical) details at lower frequencies (or larger wavelengths) or *vice versa* as explained in [6-10]. Relevantly, a π-relation $[\ell_m/\lambda_m] \Leftrightarrow [\ell_p/\lambda_p]^{\alpha}$ on similitude is framed where, the subscripts ('m' and 'p') as mentioned earlier depict the ("model" and "prototype") respectively and, α is a similitude-specific exponent.

Notwithstanding the possibilities indicated for geometrical similitude-based deductions of prototypes in EM-related exercises (such as, RCS evaluations and antenna designs etc.), only a basic method that specifies RF channel-fading *via* short-term frequency-scaling *vis-à-vis* rain-induced attenuations and signal amplitude scintillations (experienced at two different carrier frequencies) are addressed as in [27]-[28]. Further, dependence of channel characteristics across one frequency band to other is outlined in [8] in terms of envelope correlations as a function of frequency separation. Nevertheless, no exhaustive published details seem to exist on "prototypes" that describe stochastic aspects of fading channel-models and associated path-loss characteristics sought in the mm-wave/THz test-bands and inferred *via* similitude principle of low-to-high frequency-scaling using known, low-frequency details (or "models"); further, relevant considerations are also not portrayed in the contexts of MIMO-channels. Hence, objectively perceived in this study are analytic pursuits on similitude transformations of fading and path-loss characteristics of RF channels. The following two sections describe possible avenues on relevant methods.

SIMILITUDE TRANSFORMATION OF FADING STATISTICS

In wireless environment (indoor and/or outdoor), as mentioned earlier, the EM propagation inevitably encounters small- and large-scale fading observable on transreceive signal envelope. Further, the associated multipath channels and interferences encountered thereof would pose stochastic attributes to such fading. Traditionally, fading-related channel characteristics are emulated by mathematical models and statistical considerations that mimic the channel response of a fading ambient. Current methods of channel model simulations in the traditional cellular bands (UHF/microwaves) are based on "RF-in, RF-out basis". They are specified in terms of stochastic considerations pertinent to transreceive signal across the fading-channel *via* the probability distribution function, $P_\gamma(\Gamma_T)$, where Γ_T denotes a specified threshold set on the statistical variable $\gamma = (r^2/2N)$ with N being the noise power and r is the signal envelope. Summarized in Table 1 [29-38] are relevant probability distribution functions specified as regard to: (1) Rayleigh fading model; (2) Rician fading model; (3) Nakagami-m fading model; (4) generalized gamma fading model; (5) log-normal fading model; (6) logarithmically-shadowed generalized gamma (GG-L) fading model; (7) generalized Rice-lognormal (GRLN)

fading model (and its variations like Suzuki-Lorenz/Loo fading models) and (8) generalized K-fading model (and its variations).

Table 1. Fading Channel Models and the Associated Parameters [29-38].

Rayleigh fading model

$$P_\gamma(\Gamma_T) = 1 - \exp(-\Gamma_T/\gamma_o) \quad (1)$$

where, Γ_T is the specified threshold set on the variable $\gamma = r^2/2N$ with N being the noise power; r denotes the signal envelope; γ_o denotes a mean CNR namely, the (mean carrier-power)-to-(mean noise- power ratio).

Rician fading model

$$P_\gamma(\Gamma_T) = (1/2)\times\left[1 - \text{erf}\left\{-(\Gamma_T/\gamma_o - \mathcal{K}/\gamma_o)\right\}\right] + \left[\exp\left(-(\Gamma_T/\gamma_o - \mathcal{K}/\gamma_o)/\mathcal{K}/\gamma_o\right)\right]\times\left[1 - (\Gamma_T/\gamma_o - \mathcal{K}/\gamma_o)/(2\mathcal{K}/\gamma_o)..\right] \quad (2)$$

where $\mathcal{K}$ is the Rician factor; and, it denotes the ratio, [(LoS carrier-power)/(Sum of other multipath powers)]. Further, erf(.) denotes the error function.

Nakagami-m fading model

$$P_\gamma(\Gamma_T) = \left[1 - 1/(m-1)!\right]\times\Gamma_G(m, \frac{\Gamma_T}{\Gamma_o}) \quad (3)$$

where $\Gamma_G(.)$ is the incomplete gamma-function and m is related to the Rician-factor $\mathcal{K}$ as follows: $\mathcal{K} \approx [(m^2 - m)^{1/2}]/[m - ((m^2 - m)^{1/2})]$.

Generalized gamma fading model

Multipath fading channel can be modeled by three-parameter generalized gamma distribution that includes, Rayleigh, Nakagami and Weibull statistics as well as, log-normal/Suzuki fading models, as special cases. It is denoted by the following equation:

$$P_\gamma(\Gamma_T) = \left[1 - 1/(m-1)!\right]\times\Gamma_G(m, (\beta_i\Gamma_T/\Gamma_o)^{\nu_i}) \quad (4)$$

where, m_i is the fading parameter, ν_i is a shape parameter and $\beta_i = [m_i!/\nu_i]\ /[(m_i - 1)!]$.

Log-normal fading model

Large-scale path impairment tends to assume the log-normal statistics with:

$$P_\gamma(\Gamma_T) = Q\left[(1/(\Gamma_T/\gamma_o))/(\sigma_d/\gamma_o)\right] \quad (5)$$

where Q(.) denotes the complementary error function and σ_d is the standard deviation of $\ln(\gamma/\gamma_o)$, where $(\gamma/\gamma_o) = \exp\{(\sigma_d)^2/2\}$.

Logarithmically-shadowed generalized gamma (GG-L) fading model

$$P_\gamma(\Gamma_T) = 1 - \left[1/(m_f - 1)!\right]\times\left[m_f, (A\Gamma_T/\Gamma_\ell)^\nu\right] \quad (6)$$

with $m_f > ½$ being the fading parameter; further, ν is a shape-parameter, Γ_ℓ is ℓ lognormal-distributed, average signal power and, $A = [(m_f + 1)\ /(\nu - 1)]!/(m_f - 1)!$

Generalized Rice-lognormal (GRLN) channel model

$$P_\gamma(\Gamma_T) = (1/2)\times\left[1 - \text{erf}\left\{-(\Gamma_T/\gamma_o - \kappa^*/\gamma_o)\right\}\right] + \left[\exp\left(-(\Gamma_T/\gamma_o - \kappa^*/\gamma_o)/\kappa^*/\gamma_o\right)\right]\times\left[1 - (\Gamma_T/\gamma_o - \kappa^*/\gamma_o)/(2\kappa^*/\gamma_o)..\right] \quad (7)$$

This is same as in Rician model with $\mathcal{K}$ replaced by: $\kappa^* = \{[(1 + \mathcal{K}) \times (1 + \xi \times S^2)/\xi] - 1\}$ where S denotes small-scale normalized average channel power. The parameter K is the Rician contribution of diffused power component proportional to main (LoS) power component; and, ξ depicts the ratio of: (standard-deviation of the Rician power) -to- (standard deviation of the zero-mean Gaussian noise component in the channel). This model is a generalization of Suzuki-Lorenz/Loo fading channels.

Generalized gamma channel model

When both short-term power and mean carrier power (long-term) fading statistics are χ^2-distributed then the model is expressed as:

$$P_\gamma(\Gamma_T) = \frac{[2^{(\rho-1)/2}] \times [b^{(\rho+1)/2}]}{(m_{ST}! m_{LT}!)} G_{1,3}^{2,1}\left(b\Gamma_T \middle| \begin{matrix} 1 \\ \frac{\rho+2\sigma-1}{2}, \frac{\rho-2\sigma-1}{2}, 0 \end{matrix} \right) \quad (8)$$

where $G_y^x(.)$ is the Meijer G-function [32]; and, m_{ST} and m_{LT} denote respectively, the integers specific to χ^2-distribution on the number of degrees-of-freedom under small- and long-scale fading conditions. Further, $\sigma = (m_{ST} - m_{LT})$, $\rho = (m_{ST} + m_{LT} + 1)$ and $b = (m_{ST} \times m_{LT})/\gamma_o$.

Modified K-distribution channel model

Suppose dominance of stray artifacts in EM signal prevails, a modified, K-distributed statistics can be prescribed for the overall received envelope as follows:

$$P_\gamma(\Gamma_T) = 1 - \frac{(2\sqrt{\Gamma_T})^{S+2} K_{S+2}(2\sqrt{\Gamma_T})}{2^{S+1}(S+1)\Gamma(S+1)} \quad (9)$$

where S denotes small-scale normalized average channel power and $K_\alpha(.)$ is the modified Bessel functions of the second kind. This modified K-distribution model depicts the amplitude statistics of the desired signal plus unwanted artifacts of multiple Poisson statistics [29].

Deducing inferential "prototypes" of RF channels: Algorithmic steps

Pursuant to the scope of the proposed effort, suppose considering a wireless channel, its associated feature (such as, fading and path-loss) is known (experimentally or otherwise) with an explicit functional dependency in a given frequency band (f_m-band). This function is the expressed in terms of the underlying, independent variables {a, b, c, ...} as: FUNC(f_m; a, b, …).

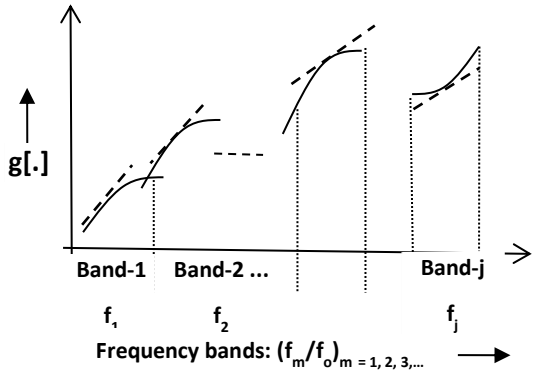

Figure 3. A hypothetical set of π-functions, {g[.]} specified across several stretches of frequency bands, (Band-1, Band-2, ..., Band-j ...); and, each g[.] is approximated by an asymptotic (piecewise linear) representation. Each frequency band is specified with a value of the normalized frequency set: $\{(f_m/f_o)_{m = 1, 2, 3,...}\}$.

The variable set $\{f_m; a, b, ...\}$ can further be expressed in a normalized form and rendered dimensionless with a corresponding set of reference values, $\{f_o; a_o, b_o, ...\}$. Each of the resulting dimensionless variable is also specified with a dimensionless exponent. In all, $FUNC(f_m; a, b, ...) \Rightarrow g[f_m/f_o; (a/a_o)^{\alpha}, (b/b_o)^{\beta}, ...]$. The function, g[.] denotes the Buckingham's π–function designated with the exponent set $\{\alpha, \beta, ...\}$.

Now, suppose a hypothetical set of π-functions {g[.]} is presumably known *ex post* relevant to a spectral range of frequencies. The function g[.] is then approximated by an asymptotic (piecewise linear) representation and attributed to represent each segmented stretch of frequency bands across the EM spectral range as shown in Figure 3. (*Note*: The bands shown need not however, be continuously and successively adjacent. There could be a window of unknown features between any two bands wherein, g[.] is unspecified).

Considering a set of successive frequency bands as illustrated in Figure 2, the EM details prescribed for each band *via* the function g[.]. That is, g[.] denotes the "models", namely, model-1, model-2, model-3 etc. respectively for the bands, Band-1, Band-2, Band-3 etc. Now, for each frequency segment of the set $\{(f_m/f_o)_{m = 1, 2, 3,...}\}$ depicting $\{(Band)_{m = 1, 2, 3,...}\}$, the associated "model" prescription can be transformed into a corresponding "prototype" of the next, (successive) higher frequency band. This is done *via* a successive iteration method using Buckingham's similitude principle as described in the pseudocode presented in Table 2.

Table 2. Pseudocode on applying similitude principle to obtain the "prototype" from the "model"

%% Given the data set on a "model" represented in π-format of channel features, known *a priori* at a (lower) frequency-band, to construct a corresponding "prototype" of those features in the next (successive) higher frequency-band iteratively by applying similitude principle

Initialize

Identify

→ Frequency spectrum with known EM characteristics

← List and tabulate all the associated variables: {a, b, c, ...}

← Select/specify appropriate reference values, $\{a_o, b_o, \ldots\}$ corresponding to the set: {a, b, c, ...}

Construct

→ A set of dimensionless variables: $\{(a/a_o), (b/b_o), \ldots\}$ segmentize the frequency spectrum with known EM characteristics to get successive frequency bands: Band-1, Band-2, … etc. located at frequencies $f_1, f_2, f_3, \ldots$, etc.

← Select/specify an appropriate reference value, f_o, to get a dimensional set: $\{f_m/f_o\}_{m = 1, 2, 3, \ldots}$ depicting the $\{(\text{Band})_{j = 1, 2, 3,}\}$

Develop

→ $\text{FUNC}(f_m; a, b, \ldots) \Rightarrow \{(\text{Band})_{m = 1, 2, 3, \ldots}\}$: Raw "model" details

← $\text{FUNC}[(f_m/f_o; (a/a_o), (b/b_o), ...)]$: "Model" function

Input

→ $\text{FUNC}(f_m/f_o; (a/a_o), (b/b_o), ...)]_{\text{"model"}}$

← π-format of the "Model" function: $g[(f_m/f_o); (a/a_o)^{\alpha}, (b/b_o)^{\beta}, \ldots)]_{\text{"model"}}$

Construct

→ For successive bands (m = 1, 2, 3, ...), specify the π-format of g[.] function

→ Example: Consider: Band-1 – Its π-format of the g[.]function:

← G1: $g[(f_1/f_o);(a_1/a_o)^{\alpha_1}, (b_1/b_o)^{\beta_1};(c_1/c_o)^{\gamma_1}, \ldots]$

→ Designate G1(.) as: Model-1

Next

→ Consider: Band-2 - Its π-format of the g[.] function

← P2: $g[(f_2/f_o); (a_2/a_o)^{\alpha_2}, (b_2/b_o)^{\beta_2};(c_2/c_o)^{\gamma_2}, \ldots]$

→ Designate P2(.) as: Prototype-2

Apply

→ Apply Buckingham's similitude principle

Equate

← Band-1 - π-format of the g[.] function: G1(.) and Band-2 - π-format of the g[.] function: P2(.)

← $g[(f_1/f_o); (a_1/a_o)^{\alpha 1}, (b_1/b_o)^{\beta 1};(c_1/c_o)^{\gamma 1}, \ldots]$

≡ $g[(f_2/f_o); (a_2/a_o)^{\alpha 2},(b_2/b_o)^{\beta 2};(c_2/c_o)^{\gamma 2}, \ldots]$

Next

Deduce

→ $[k_2 \times P1(f_2/f_o)]^{C_2}$

← This is a scaled version of $[k_1 \times G1(f_1/f_o)]^{C_1}$ with (k_1/k_2) as a scaling constant and $\{C_1$ and $C_2\}$ being the exponents that decide a power-law relation

⇒ Prototype-2 of Band-2

Next

→ Use Prototype-2 as a pseudo- "model" for prototyping Band-3

→ Consider: Band-2 – π–format of the g[.] function

← P2: $g[(f_2/f_o); (a_2/a_o)^{\alpha 2}, (b_2/b_o)^{\beta 2};(c_2/c_o)^{\gamma 2}, \ldots]$

→ Rename P2(.): Prototype - 2 as: Pseudo-model-2

→ Consider: Band-3 - π-format of the g[.] function

← P3: $g[(f_3/f_o); (a_3/a_o)^{\alpha 3}, (b_3/b_o)^{\beta 3};(c_3/c_o)^{\gamma 3}, \ldots]$

→ Designate P3(.) as: Prototype-3

Next

Equate

→ Band-2 - π-format of the g[.] function: P2(.) and Band-3 - π-format of the g[.] function: P3(.)

→ $g[(f_2/f_o); (a_2/a_o)^{\alpha 2}, (b_2/b_o)^{\beta 2};(c_2/c_o)^{\gamma 2}, \ldots]$

≡ $g[(f_3/f_o); (a_3/a_o)^{\alpha 3}, (b_3/b_o)^{\beta 3};(c_3/c_o)^{\gamma 3}, \ldots]$

Deduce

→ $[k_3 \times P3(f_3/f_o)]^{C_3}$

→ This is a scaled version of $[k_2 \times P2(f_2/f_o)]^{C2}$ with (k_2/k_3) being a scaling constant; and, $\{C_2$ and $C_3\}$ are the exponents that decide the associated power-law relation

⇒ Prototype-3 of Band-3

Next

→ Use Prototype-3 as a pseudo-model for prototyping Band-4

← (and so on …)

Continue

→ Iteration until the entire spectrum of interest is exhausted

List

→ "Prototypes" evolved across the entire spectrum of interest

%% *Comment*: The above procedure allows elucidating the features in a given band, say, Band- M, by knowing the features in the previous band, Band (M – 1) *via* scaling and similitude principle.

→ That is, the features of Band (M – 1) depict the known *ex post* profile or the "model"; hence, the unknown profile of the Band-M inferred *ex ante* depicts the desired "prototype"

End

Ascertaining "prototypes" of channel models in the desired spectral range (of mm-wave through THz band stretching into suboptical regions) following the procedure described above,

would allow assaying relevant composite fading-channel characterizations. Such channel-models will permit comprehending several physical issues in wireless communications including interference effects in MIMO networks, distributed antenna systems and cooperative/multi-hop relay networks. As well known, in a typical signal propagation scenario, the received signal typically will show fading consisting of very rapid fluctuations around the mean signal level superimposed on relatively slow variations of the mean level. Therefore, it will be inconsistent to assume that the local mean power of the multipath fading is a random variable (RV) distributed over $(0, \infty)$ as per traditional lognormal and/or gamma distributions.

For example, in mm- and sub-mm wave band, non-LOS propagations, the standard deviation of shadowing could be larger than in the contexts of cellular communication (at 5 GHz [1-2]) due to shadowing cast by stationary and/or moving objects. Relevantly, signal power can be significantly lost (up to 20 dB), if the LOS component is blocked by an object and this is much realistic in millimeter/sub-mm wave environment. However, diffraction effects (due to EM field behind the obstacle) in the test bands could be much smaller in comparison with lower band, 5 GHz propagation. That is, shadowing zones are markedly very sharp in mm/sub-mm frequencies.

In short, the ambient changes could occur very fast (with respect to the diversity and average power of the received signal) in the test bands of interest. In addition, towards suboptical spectrum deployed in free-space communications, the atmospheric turbulence that originates from variations in the refractive index of the transmission medium (as a result of inhomogeneities in temperature and pressure changes) will increase the standard deviation of shadowing on channel fading As a result, the identification of a tractable probability density function (PDF) to describe the physical problems at the background of shadowing effects is important in order to study the performance characteristics of emerging and future wireless communication systems operating in those EM environments. Corresponding envelope and the power of the received signal (in the test bands across millimeter/sub-millimeter wave regime and in free-space sub-optical channels), the first and the second-order statistics of the received signal envelope need to be "prototyped" with appropriate "model" details characterized by the so-called extended generalized-K (EGK) model of composite fading distribution [39]. That is, notwithstanding the typical model-to-prototype depictions of channel models indicated in Table 1, the EGK model and its special cases as listed in [39], appear to be closely appropriate candidates for applications in the test bands under discussion.

Constructing a "prototype" of a fading channel-model: An illustrative example

Fading characteristics as a function of frequency can be expressed in terms of the statistics of RF signal envelope *versus* frequency separation *via* correlation parameters as indicated in [40]. However, in similitude exercises toward deducing a "model"-based inferential "prototype" along a desired frequency-scale, is not *per se* to find a 'statistical correlation' between the "model" and the "prototype", but to seek a 'similarity' between them. That is, the EM/channel characteristics at different bands of frequencies need not necessarily be 'statistically correlated'; and, relevant similitude exercise of interest is to find rather a 'similarity of details' between them.

Relevantly, suppose the similarity of fading phenomenology across the frequency bands of a "model" and its "prototype" is to be ascertained. The prime fading-related variables of interest

pertinent to fading channel-models are enumerated in Table 2 where fading statistics is modeled in terms of the RF power-content of the link relative to the channel noise power; hence, the associated stochastic aspects are denoted *via* fluctuating envelope statistics of the signal transits across the transceiver path [29]-[38].

For example, suppose a channel-model (like Rayleigh, Rician etc.) is specified in terms of the associated carrier-to-noise (power) ratio (CNR) expressed as: $\gamma = r^2/2N$ (with r being the signal envelope and N is the noise power). Then, its corresponding fading statistics (specified in terms of probability density function) can be availed (as in Table 1) and it leads to specifying the probability, $P_\gamma(\Gamma_T)$ that, γ does not exceed a specific threshold value, Γ_T. Now, denoting the mean CNR by γ_o (namely, the mean carrier-power to mean noise-power ratio), $P_\gamma(\Gamma_T)$ can be ascertained in normalized dimensionless formats, ready for similitude applications; and, the method of transforming "the model" into a corresponding "prototype" can be pursued as illustrated in Figure 3 and as outlined below.

Considering a given fading channel, suppose f_1 and f_2 are two carrier frequencies in two independent spectral ranges, say, in Band-1 and Band-2 respectively and, a similitude relation is sought between these two bands. That is, given a known extent of mean CNR at f_1 namely, $\gamma_o|_{f1}$, its corresponding value at f_2 namely, $\gamma_o|_{f2}$ can be obtained *via* π-relation prescribed with appropriate power-law exponent sets $\{\alpha_1, \beta_1\}$ and $\{\alpha_2, \beta_2\}$ on the variables for example, as shown below in equation (10) as regard to a Rayleigh channel. (Here, the relevancy of linear, undistorted similitude principle is implicitly assumed as well as, the statistical features of CNR across Band-1 and Band-2 are considered to be 'similar', but not necessarily 'correlated'; and as such, they are statistically independent).

$$\left[\frac{(\gamma_o|_{f_1})^{\alpha_1}}{(\gamma_o|_{f_2})^{\alpha_2}}\right] = \left[\frac{(\Gamma_{T_1})^{\beta_1}}{(\Gamma_{T_2})^{\beta_2}}\right] \times \left[\frac{\log_e\left(\frac{1}{1-P_\gamma(\Gamma_{T_1})^{\beta_1}}\right)}{\log_e\left(\frac{1}{1-P_\gamma(\Gamma_{T_2})^{\beta 2}}\right)}\right] \qquad (10)$$

where $P_\gamma(\Gamma_T)$ is explicitly given for Rayleigh channel in Table 1; and, the subscripts (1 and 2) explicitly define pertinent details of Band-1 and Band-2 respectively. Likewise, given the power-form (CNR) statistics of any other established channel models as listed in Table 1, the corresponding, $[(\gamma_o|_{f1})^{\alpha 1}/ (\gamma_o|_{f2})^{\alpha 2}]$ version of π-form relation can be determined, so as to deduce the fading slope of the "prototype" *vis-à-vis* the "model".

INFERRING THE PATH-LOSS *VIA* MODEL-TO-PROTOTYPE SIMILITUDE

Apart from fading channel characterizations, the RF channels can also be studied in terms of the extent of power-loss across the channel. It implies usable RF power (or field strength) that can robustly deliver the required signal-level for reception with a specified integrity. Relevantly, the archival data that exists in the literature [4-8] offers a gist of so-called "path-loss models". They describe the extent of RF power-loss budgets under various ambient (outdoor as well as, indoor) mostly as a function of transreceive distance at various frequencies, HF through UHF/microwave frequencies. Typically, commencing from a simple free-space model, such path-loss characteristics in outdoor contexts are addressed by duly accounting the

penetration losses due to atmospheric/tropospheric contents and terrain features. For example, in the so-called Longley-Rice model [41], the terrain path profile and area mode across irregular turfs are considered in path-loss predictions across 20 MHz to 10 GHz spectrum.

Likewise, the so-called Okumura model [42] does signal prediction in urban areas in the frequency range 150 – 2000 MHz and distances 1-100 km, taking antenna heights into consideration; and, the Hata model [43] enables a graphical solution on path-loss information concerning urban area. Further, the RF signal-strength and path-loss predictions due to Walfish and Bertoni model [44] account for the impact of rooftops and building heights, (*via* diffraction theory). Classical multipath propagation model with statistical considerations is presented in [45].

Concerning indoor RF propagations, the channel is characterized by Hashemi model as in [46] and electromagnetics of radio propagation within buildings is addressed in [47]. Further, the statistical channel impulse-response models on radio communications (due to Rappaport et al. [48]) that enclave the factory and open-plan building ambient exist and are labeled as the SIRCIM model. More supplementing details pertinent to indoor RF channel-models are due to Saleh and Valenzula [49]; further, Seidal and Rappaport have presented UHF path-loss models concerning multi-floored indoor propagations in [50]. Concurrent to possible path-losses in indoor RF propagations considering multiple reflections and clustered contents in confined spaces, inevitable interferences may also possible due to coexisting services. Relevant considerations are addressed by the author and others in [51].

Channel path-loss implies incurrence of attenuating signal power along its transreceive transits. For example, EM energy losses on terrestrial paths across open-terrains arise as a result of: Isotropic and directional distance (R) dependent, free-space (1/R)-losses, transmission media (material) penetration/scintillation losses and RF-signal power degradations due to reflection, scattering, diffraction, shadowing etc.; and, in indoor premises the RF power-losses may occur due to fading (of frequency/time/spatial versions), depolarization effects, mobility-specific signal-path attributes (due to Doppler spread), propagation delays, RF-system specific considerations and signal artifacts caused by co- and adjacent channel interferences.

In general, suppose P_R is the received signal power and P_T is the transmitted power, then P_R/P_T refers to the power-loss expressed as $[10 \times \log_{10}(P_R/P_T)]$ in decibels (dB); and, for omnidirectional free-space wave front, the dimensionless format of similitude relation, $[P_R/P_T] = [(R/\lambda)/(R_o/\lambda)]^{\alpha 1}$can be specified, where R is the transit distance, R_o is a reference distance, λ is the wavelength of EM energy and α_1 is a path-loss exponent (typically, close to 2). For various other path-losses indicated above, $[P_R/P_T]$ can be deduced likewise in dimensionless forms and specified with varying extents of the path-loss exponent, as necessary.

Notwithstanding the status that path-loss characterizations have been evolved largely in the classical EM scenario pertinent to HF through microwave spectrum (and sparsely in the mm-wave band), no comprehensive path-loss modeling seems to exist *per se* to depict the relevant profiles in the test ranges of sub-mm through THz band; and, specifically, such comprehension is totally absent (or inadequate, if it exists) for MIMO-channels in the said test bands. Therefore,

suggested here is to invoke the thematic of Buckingham's similitude principle to deduce the "prototypes" of path-loss characteristics at the desired test bands *vis-à-vis* corresponding known details of the "models" in the available stretches of lower-end frequency bands.

Hence, commensurate with the objective as above, the model-to-prototype transformation as needed, a compatible set of path-loss functions (PL1 through PL9) can be formatted in dimensionless forms as listed in Table A.1 wherein, the pertinent details include both LoS and non-LoS transmissions across single- and/or multi-path signal transits, each path possibly posing unique angle-of-arrival (AoA).

Constructing a "prototype" of a path-loss-model

The underlying concept of similitude-based scaling of path-loss up into higher frequency spectra can be specified *via* "model"-to-prototype transformation. Using the relevant path-loss ratio, PLR (= P_R/P_T) functions indicated in dimensionless forms in Table A.I, the underlying similitude consideration can be illustrated with the following illustrative example (of Figure 4):

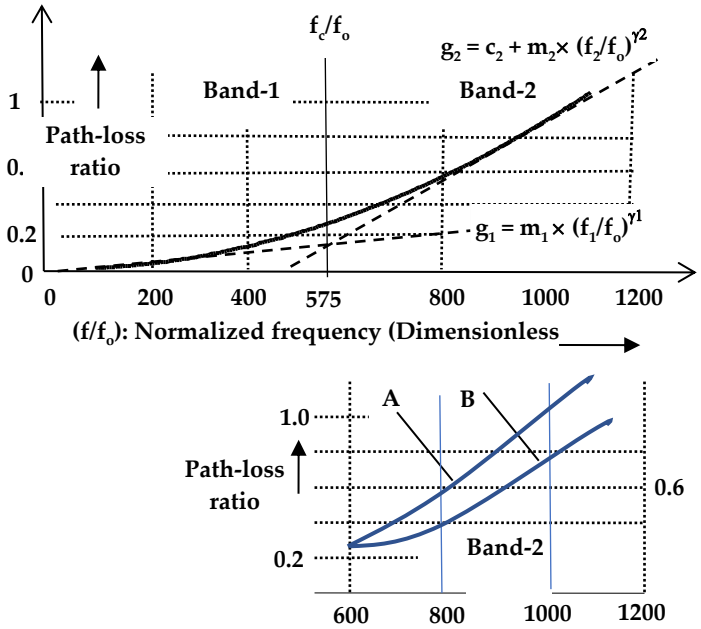

Figure 4 A typical, relative path-loss ratio profile expressed as RF power attenuation (per km) *versus* frequency (from 5 GHz through 1000 GHz with f_o: Normalization (reference frequency) = 900 MHz [52]. (A: Actual measured data as in [52] and B: Inferred data as per linearized similitude principle; Band-1 and Band-2 are designated spectra on either side of the corner frequency, f_c/f_c = 575 and similitude-based inference is made in Band-2).

Suppose as an example, the data available in [52] on attenuation (per km) *versus* frequency range up to 1000 GHz (normalized with a reference frequency, f_o = 900 MHz) is plotted as illustrated in Figure 4 (pursuing band-by-band segmentation strategy indicated in Figure 3). In Figure 4, the profiles of path-loss *versus* decades of frequency changes are shown for the bands, (Band-1 and -2). There are two asymptotes marked (in dotted-lines) with a point of intersection at a corner frequency, f_c/f_o = 575. Now for analysis, the left-side of f_c/f_o taken as Band-1 representing the *ex post* details of the "model": FUNC(Band-1) ≡ $[(\text{Path-loss})_{\text{Band-1}}]$; and, the

right-side is the Band-2 denoting the *ex ante* details to be framed by realizing a "prototype": FUNC(Band-2) ≡ [(Path-loss)$_{\text{Band-2}}$] *via* similitude considerations.

Suppose, the corresponding π-relations are specified as $g_1(.)$ and $g_2(.)$ for Band-1 and -2 respectively. Explicitly, considering the bands, Band-1 and -2, the linear asymptotes that can be prescribed are: $g_1=[m_1 \times (f_1/f_o)^{\gamma_1}]$ and $g_2=[m_2 \times (f_2/f_o)^{\gamma_2} + c_2]$, where f_1 and f_2 denote any representative frequency variable in Band-1 and -2 respectively; and, the set $\{\gamma_1, \gamma_2\}$ depicts the corresponding exponents assigned to the dimensionless (normalized) variables, (f_1/f_o) and (f_2/f_o). Further, m_1 and m_2 represent the slopes of the asymptotes estimated in the *ex post* regime, typically at f_c/f_o; and, c_2 is the dimensionless y-intercept of the asymptote in Band-2. Hence equating, $g_1(.)$ and $g_2(.)$ on similitude basis, and assuming $\gamma_1 = 1$ as a reference, the relative value of γ_2 can be deduced as follows:

$$\gamma_2 \text{ (relative to } \gamma_1 = 1) = \{\log_{10}[m_1 \times (f_M/f_o)]\}/\{\log_{10}(m_2 \times [(f_M/f_o) - (f_c/f_o)] + c_2)\} \qquad (11)$$

where (f_M/f_o) represents a projected *abscissa* value. It is approximately taken as the mean of: (f_c/f_o) and the maximum (f_2/f_o) of interest in Band-2. Thus, the function denoting the path-loss ratio in Band-2 (*ex ante* regime) can be inferred *via* $g_2(.)$.

Pertinent to the numerical example for the data indicated in Figure 4, the calculated values are: $m_1 = 5.043 \times 10^{-4}$; $m_2 = 1.473 \times 10^{-3}$; $(f_c/f_o) \approx 575$; $(f_M/f_o) = 843$; γ_2 (relative to $\gamma_1 = 1$) = 2.2597; and, $c_2 = 0.29$. Hence, plotted as the *ex ante* deduction in Band-2, is the curve, B depicting the inferred value of path-loss ratio *versus* frequency (f_2/f_o); and, co-presented curve A represents the prior known data for the same frequency regime as available in [52]. That is, curve A is indicated to cross-validate the inferred curve B. Presented in Table 2 are relevant numerical values of relevant curves in Figure 4.

The heuristics of the approach as above relies on linear similitude considerations. However, as said earlier, the EM propagation characteristics may be such that, the similitude implemented could be of 'distorted type'. Nevertheless, the frequency bands are segmentized (as Band-1, Band-2 etc.), and in each segment, the functional variation of channel characteristics *vis-à-vis* frequency (all in dimensionless □-format) can be regarded as asymptotically (piecewise) linear as illustrated in Figure 3; and as such, successive "power-law" predictions from model-to-prototype is assumed to hold water. More examples in framing model-to-prototype transformations of path-loss characteristics, are presented in the following subsection.

Table 3. Relative path-loss ratio: Measured empirical data [52] *versus* values inferred *via* similitude principle

	Path-loss ratio	
f_2/f_o	Actual data [52]	Inferred values
600	0.31	0.29
650	0.36	0.29
700	0.42	0.31
750	0.49	0.34
800	0.55	0.37
850	0.63	0.42
900	0.70	0.48
950	0.78	0.60
1000	0.87	0.64
1050	0.96	0.74
1100	1.05	0.90

Exemplars of lower frequency band "models" of path-loss characteristics

Pursuing the procedure indicated with an example above, the art of similitude adopted towards framing the model-to-prototype transformations of path-loss characteristics, the following examples of lower frequency band "models" are indicated to obtain their corresponding prototypes.

A. Lee's model [5]

This path-loss model suggests an asymptotic variation in path-loss across decades of frequency changes as illustrated in Figure 5. For example, suppose, the attenuation *versus* frequency is specified and known in the range up to 1000 MHz (denoted as Band-1).

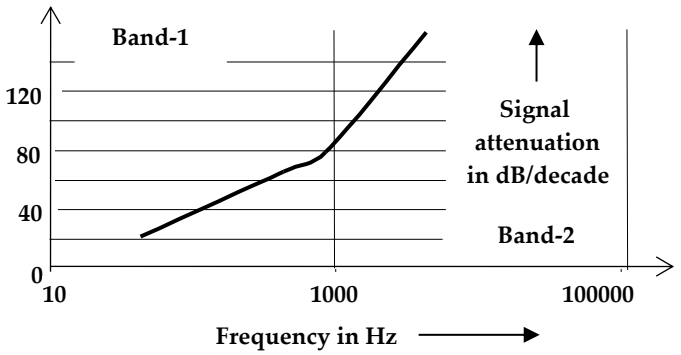

Figure 5. Lee's model [5]: An example depicting the change in signal attenuation (expressed in terms of the slope dB/decade) over a range of: 40 MHz through 4000 MHz observed in the path-loss profile. The data is specified within the radius of coverage based on radio horizon distance and base-station antenna height under non-obstructive point-to-point RF transits.

The signal attenuation (in dB/decade) shown represents a "model": $\text{FUNC}(f_{1\text{-band}};\ \alpha_1) \equiv [(P_R/P_T)_{f1\text{-band}}]^{\alpha 1}$. Relevantly, the EM power-loss is regarded mainly due to free-space, far-field EM wave proliferation; as such, it follows the (1/R)-law (as limited by antenna-beaming considerations). (However, in the event of EM absorption *versus* frequency due to path-

constituents and terrain-specific scattering details exist, relevant EM similitude prospects of EM propagation will refer to a more lossy and dispersive ambient as addressed in the classical efforts of [22]).

B. Okumura's urban model [42]

In the case of patterned/beamed EM illuminations of an area with associated transit-path absorptions and terrain-specific attenuations, the similitude modeling can be prescribed *via* Okumura model [42]. Relevant to this EM ambient, the modeling refers to elucidating frequency *versus* median attenuation experience over quasi-smooth terrains in an urban area. Corresponding dimensionless format of the gross path-attenuation specific to a "model" at a given carrier frequency, f_m can be formulated as follows: Suppose an observation locale is at R from an RF source and a reference distance is specified as R_o (normally taken as 1 mile or 1600 meter). Then, the "model"-function at a frequency, f_m can be written as follows:

$$[P_R(R/\lambda_m)/P_o(R_o/\lambda_m)] = [(R/\lambda_m)/(R_o/\lambda_m)]^{-\kappa_1} \times [(h_T/\lambda_m)/(h_R/\lambda_m)]^{-\kappa_2} \times [(\lambda_o/\lambda_m)]^{-\kappa_3} \\ [\{\exp(-a_{1m}(R/\lambda_m)/(R_o/\lambda_m)\}^{(\kappa_4)_A} \times \{\exp(-a_{2m}(R/\lambda_m)/(R_o/\lambda_m)\}^{(\kappa_4)_T}] \quad (12)$$

where, (λ_o) depicts a reference wavelength of measurement, (say, at $f_o = 900 \times 10^6$ Hz) and its corresponding wavelength in meters; (h_T and h_R) represent the transmitter and receiver antenna heights respectively.

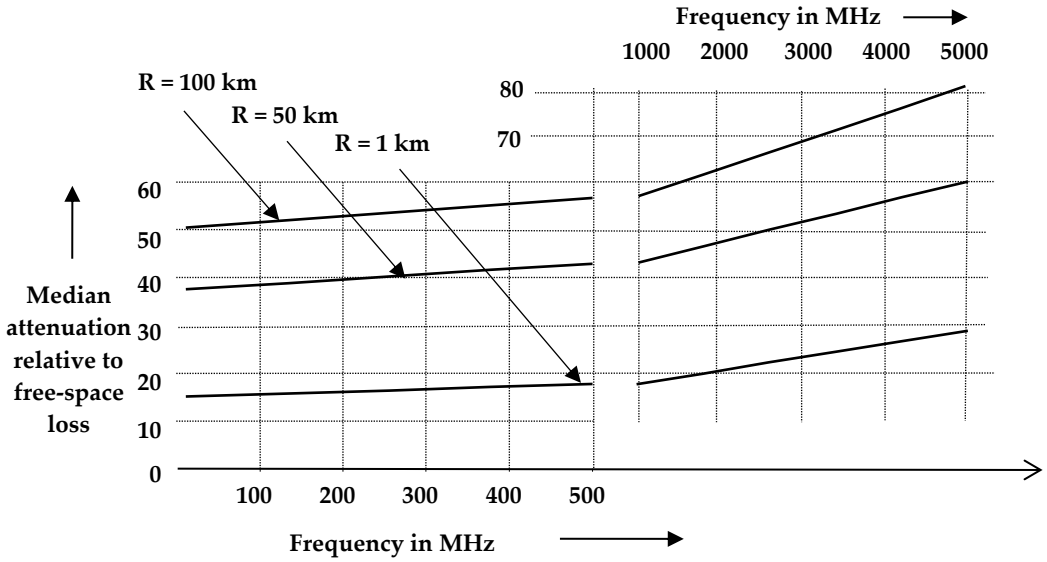

Figure 6: Okumura model: A typical example of frequency *versus* asymptotes of median (EM) attenuation experienced over a quasi-smooth terrain in an urban area - (based on results as in [5] for a mobile unit antenna height 3 m and a base-station antenna height of 200 m).

The model exponents are: $\{\kappa_1, \kappa_2, \kappa_3, \kappa_4\}$. Further, the coefficients a_{1m} and a_{2m} denote the absorption (A) and terrain-specific (T) effects respectively. In a dimensionless form, they are given by:

$$[a_{1m}]_{\text{"Model" at } f_m} = \left[\begin{array}{l} (2\pi \times \lambda_o / \lambda_m) \times [0.5 \times (\mu / \mu_o) \times (\varepsilon / \varepsilon_o) \times \{1 + \\ \qquad [(\sigma / \sigma_o) / (2\pi \times f_m / f_o) \times (\varepsilon / \varepsilon_o)]^2\}^{1/2} - 1]^{1/2} \end{array} \right]$$

and

$$[a_{2m}]_{\text{"Model" at } f_m} = [(d_T / d_m) / (d_o / \lambda_o)] \quad (13)$$

where d_o and d_T denote the Rayleigh-criterion specified on terrain irregularity (shape) across R_o and R_T respectively; and, σ/σ_o depicts the normalized conductivity responsible for the EM absorption in the medium.

Now, the scaling of equation (13) can be done *via* similitude principle to get the "prototype" at a desired elevated frequency $f_p >> f_m$ as follows: For the "prototype" being elucidated at f_p:

$$[P_R(R/\lambda_p) / P_o(R_o/\lambda_p)] = [(R/\lambda_p)/(R_o/\lambda_p)]^{-\zeta_1} \times [(h_T/\lambda_p)/(h_R/\lambda_p)]^{-\zeta_2} \times [(\lambda_o/\lambda_p)]^{-\zeta_3} \times [\{\exp(-a_{1p}(R/\lambda_p)/(R_o/\lambda_p)\}^{(\zeta_4)_A} \times \{\exp(-a_{2p}(R/\lambda_p)/(R_o/\lambda_p)\}^{(\zeta_4)_T}] \quad (14)$$

where the subscripted index 'p', as stated before denotes the "prototype" considerations applicable at f_p with the prototype exponent set being: $\{\zeta_1, \zeta_2, \zeta_3, \zeta_4\}$. The normalized set of parametric data in equations (13) and (14) are:

$$\{P_R(R/\lambda_{m \text{ or } p}), P_o(R_o/\lambda_{m \text{ or } p}), (h_T/\lambda_{m \text{ or } p}), (h_R/\lambda_{m \text{ or } p}), (\lambda_o/\lambda_{m \text{ or } p}), a_{1\,m \text{ or } p}, a_{2\,m \text{ or } p}\} \quad (15)$$

These entities and the exponents indicated enable formulating the required similitude of "model" -to- "prototype" function transformation concerning the path-attenuation under consideration.

With reference to a typical Okumura path-loss model presented in Figure 6, there are three observable aspects on path-loss characteristics. Relevant path-loss slope varies over the decades of frequency, the path distance (R) and EM propagation across more than one type of environment. In essence, the variation of path-loss *versus* decades of frequency is indicated by varying path-loss slope for a given antenna height ratio and transceive distance. Thus, the results in Figure 6 depict segmented asymptotic variations across some (Band-1)-to-(Band-2). Hence, corresponding pair of, "model": $\text{FUNC}(f_{1\text{-band}}; \alpha_1) \equiv [(P_R/P_T)_{f1\text{-band}}]^{\alpha 1}$ and a "prototype": $\text{FUNC}(f_{2\text{-band}}; \alpha_2) \equiv [(P_R/P_T)_{f2\text{-band}}]^{\alpha 2}$ can be inferred *via* similitude considerations.

C. Medium-specific absorption losses – Crane model/JPL model on rain-attenuation [53-55]

Precipitation (rain, snow and fog specific) losses are highly dependent on seasonal variations, rain structure and rain-rate statistics [43], and conform to outdoor EM absorption resulting from dielectric losses. The extent of such losses per unit distance will depend on the density and dispersive pervasion of absorbing (lossy) contents being present; and, such lossy dielectric-based EM absorption is also approximately proportional to the square of the frequency of the propagating wave. Further, the vertical structure as well as, the rain cell-size would play significant role in making of a relevant global attenuation model. Typically, the so-called Crane attenuation model is an exemplary depiction, which duly accounts for the parameters on the path-length (R), rain-rate, rain-height, rain- volume etc. over typical sets of terrains.

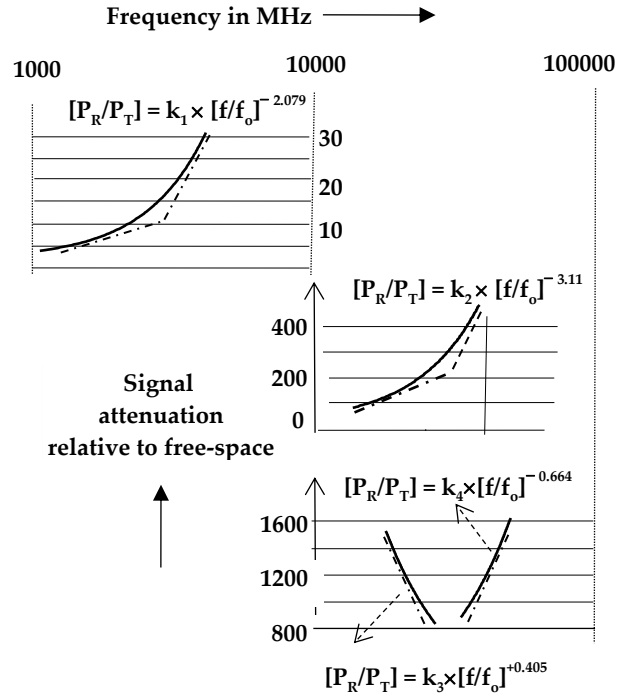

Figure 7. JPL model: An exemplar of Zenith attenuation *versus* frequency [56] compared to free-space loss across R = 100 km. The underlying SHF band (3 GHz and 30 GHz) propagation refers to a medium with oxygen and water-vapor (of density 7.5 g/m^3). Note a maximum attenuation around 20 GHz and then a fall-off.

Measurements and models of Jet Propulsion laboratory (JPL) [53-55] exemplify the estimation of microwave power margin losses due to atmospheric conditions with amplitude scintillations across turbulent atmosphere [56] and rainfall climates; and, the path attenuation is indicated as being consistent with log-amplitude fluctuations. Further, rain-specific path-loss can be regarded as a superposition on rain-free propagation path-loss weighted by a ratio of variances $[(V(f_1)/V(f_2)]$ at two frequencies f_1 and f_2 (with corresponding wavelengths λ_1 and λ_2) That is, $[P_R(R)/P_T(R)]_{\text{Rainy medium}} = [P_R(R)/P_T(R)]_{\text{Rain-free medium}} \times [V(f_1)/V(f_2)[\times [(\lambda_1/\lambda_2)^{\nu}] \times$ (a function decided by: height of turbulent layer, angle of elevation, air radius, antenna parameters); and, the exponent ν is a constant for a given medium. Figure 7 corresponds to the empirical data adopted from the results in [53-55]. Again considering a "model": $\text{FUNC}(f_{1\text{-band}}; \alpha_1) \equiv [(P_R/P_T)_{f1\text{-band}}]^{\alpha 1}$ inference on a "prototype": $\text{FUNC}(f_{2\text{-band}}; \alpha_2) \equiv [(P_R/P_T)_{f2\text{-band}}]^{\alpha 2}$ can be accomplished *via* similitude considerations.

D. Foliage attenuation specified absorption-based path-losses [57-58]

Lossy influence of vegetation and foliage on EM wave propagation is inevitable [57]; and, such vegetation effects on path-loss in mobile cellular communication could be significant as indicated in [58]. Typical such path-loss variation (Figure 8) for a given transmitter receiver set of heights and path distance can be specified with the approximate measured data collected in a specified environment [58]. Relevantly, a transformation of a "model": $\text{FUNC}(f_{1\text{-band}}; \alpha_1) \equiv [(P_R/P_T)_{f1\text{-band}}]^{\alpha 1}$ to infer a "prototype": $\text{FUNC}(f_{2\text{-band}}; \alpha_2) \equiv [(P_R/P_T)_{f2\text{-band}}]^{\alpha 2}$ *via* similitude considerations is feasible.

Figure 8 illustrates an example of measured path-loss asymptotes (relative to free-space path-loss) over a foliage-infested terrain. Thus, the *ex ante* predictions of the path-loss characteristics in a desired higher ranges of frequency spectrum can be done using the *ex post* details on known path-loss features available in the lower strata of EM spectrum.

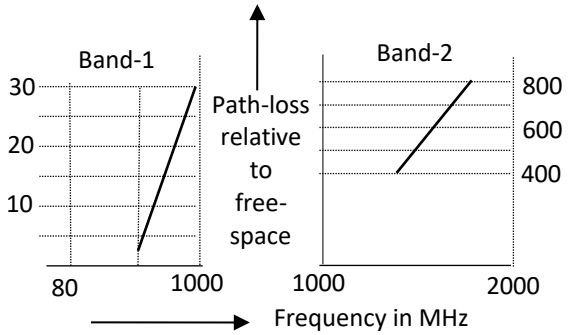

Figure 8 An example of measured path-loss asymptotes (relative to free-space path-loss) with vertical polarization with antenna height ratio of (h_T/h_R) = 35 across R = 500 m range over a foliage-infested terrain.

Pertinent set of path-loss descriptions indicated in the Appendix I (Table A.1) are as follows: PL1: RF transit-paths losses across isotropic (and directional) along the distance R; PL2: Penetration and scintillation losses in the transmission media (material); PL3: RF-signal power degradations due to reflection, scattering, diffractions, and/or shadowing or blocking phenomena across open-terrains/indoor premises in the LoS and/or non-LoS, multipath transits: Reflection, scattering, diffraction or shadowing specific terrain- or indoor-based EM losses; PL4: Fading (frequency/time/spatial) specific RF power-losses– Fading (frequency/time/spatial) associated RF power-losses in outdoor and indoor settings; PL5: RF-power loss *versus* depolarization (intentional and/or unintentional) effects) - EM wave depolarization effects; PL6: Transceiver mobility-specific path-loss attributes due to Doppler spread (Doppler-shift in carrier frequency); PL7: Transceiver site-specific power-delay profile *versus* path-loss characteristics: RF power-delay *versus* path-loss characteristics and PL8: Power-loss due to the antenna beam-shape or lobing, collapsing losses (caused by diversity etc.), RF system-specific filter losses and defocusing effect. Indicated in [59] is a method on path-loss characterization *via* numerical assessments for GHz channels. Relevant results are considered to evolve state matrices of short-range communications across MIMO channels and a model for THz channel is deduced thereof.

INFERENTIAL REMARKS AND DISCUSSIONS

In essence, the inferred outcomes of this study can be briefly listed as follows:

- Feasibility of deducing RF channel/EM propagation characteristics ("prototypes") in a desired higher spectral range of frequency using the available knowledge ("models") in the lower strata of EM spectrum
- Using the Buckingham's theorem on similitude principle [3] and judiciously applying it to the RF channel-modeling framework of transforming a "model" to a "prototype"
- Formulating necessary Buckingham's π-relations in the contexts of EM problems outlined in terms of dimensionless setting of EM entities

- Making a "prototype" of a fading-channel from the existing "model" details pertinent to established CNR-specific statistical fading distributions
- Using a known path-loss *versus* a lower-end frequency-band, relevant *ex post* "model" is transformed to *ex ante* path-loss details ("prototype") in the upper-side frequency-band.
- Attributing any deviations in the inferred "prototype" *versus* the actual data to asymptotic linear approximation made on the underlying 'distorted' similitude profile.

Shortcoming of similitude approach

The heuristics of the approach pursued in this study relies on linear similitude considerations. However, EM propagation characteristics may be such that, the similitude implemented could be of 'distorted type'. Nevertheless, as assumed here, the frequency bands are segmentized (as Band-1, Band-2 etc.), and in each segment, the functional variation of channel characteristics *vis-à-vis* frequency (all in dimensionless ?-format) can be regarded as asymptotically (piecewise) linear as illustrated in Figure 3; and as such, successive "power-law" predictions from model-to-prototype may hold water to a reasonable extent. However, refinement to the algorithms can be pursued as indicated below.

Refining the similitude approach to overcome the shortcomings

The similitude considerations on 'distorted type' model-to-prototype conversion though can be assumed as 'asymptotically (piecewise) linear' across the power-law relations between successive inferential predictions, further refinements to the algorithms are possible by:

a) Elucidating the relative entropy (or loss of information, in Shannon's sense) while converting the 'distorted' function to a 'linear' asymptote
b) Deducing model-to-prototype (inter-model) variability through appropriate weighting and scaling corrections and determining EM-scenario variations (uncertainty) across band-to-band (Figure 2) segments. This amounts to finding the inter-scenario relational coefficients
c) Determining risk-evaluation models with statistical bounds in the probabilistic framework of EM/RF channels and while exercising the Buckingham's principle
d) Developing *ad hoc* decision-theoretics on model-to-prototype deductions

The aforesaid tasks are open-questions indicated here as viable suites for future studies.

CLOSURE

The present and future prospects of terahertz communications are portrayed in [60]-[62]; and, commensurate with the sprouting of 5G for next-generation wireless communications, the associated paradigm shifts in research are seen largely inclined towards the inevitable use of mm-Wave stretching into sub-mm wave band and into the THz spectral domain [62]. Consistent with the scope of inferring the EM channel characteristics in such unexplored frequency bands, indicated in this study are neoteric basics of relevant feasibility considerations in applying Buckingham's theorem of similitude principle. Apart from the traditional applications of geometric similitude efforts indicated in EM contexts (of antenna designs and RCS studies etc.), the dynamic similitude considerations relevant to EM propagation presented here and developed specifically to assess the fading channel and path-loss characteristics at desired higher-end frequency (test) bands of interest are novel. In essence, this study shows new method(s) and feasibility aspects of transforming the existing knowledge (or "model") of EM

characteristics in the lower strata of EM spectrum into similitude details (of a "prototype") across a desired test frequency-band. However, it is emphasized the underlying method is quasi-analytic and empirical to a certain extent. Nevertheless, exhaustive results on deducing such "prototypes" of fading-channel statistics and channel path-loss profiles are evolved here. To the best of authors' knowledge, no equitable studies/results seem to prevail in open-literature.

APPENDIX A

Table A1: Types of path-losses and algorithmic representations of path-loss ratio (PLR) expressed in π-format

Types of path-losses and descriptions
PL1: RF transit-paths losses across isotropic (and directional) along the distance R
It refers to EM energy fall-off across its proliferation in free-space. Denoted as the ratio: Received power (P_R) /Transmitted power (P_T), the path-loss ratio (PLR) is specified as follows: For omnidirectional path: PLR = $[P_R / P_T] = [(R/\lambda)/(R_o/\lambda)]^{\alpha_1}$ (A1.1) R/R_o: Ratio - (Transit distance/reference distance) PLR: $10 \times \log_{10}$(PLR) expressed in decibels (dB): α_1: Exponent for omnidirectional propagation. (For free-space, $\alpha_1 \approx 2$) (λ): Carrier wavelength For antenna-directed path: $[P_R / P_T]_{PL1} = [(R/\lambda)/(R_o/\lambda)]^{\alpha_1} \times [(A_{eT} A_{eR} \rho_T \rho_R)/\lambda^4]^{\alpha_2}$ (A1.2) R/R_o: (Transit distance/reference distance) α_2: Model-specific exponent for the directed path {A_{eT}, ρ_T} and {A_{eR}, ρ_R}: {Antenna aperture size, radiating efficiency} of transmitting and receiving antennas.
PL2: Penetration and scintillation losses in the transmission media (material)
Relevant media-dictated penetration losses occur due to EM absorption (ABS) by material contents and scintillation-effects across turbulent atmosphere (TS) over the distance, R Absorption-related, PLR: $[P_R / P_T]_{PL2(ABS)} = [AS_{ABS}\{\exp(-a_1 R/\lambda)\}^{(\alpha_3)_1} \times \{\exp(-a_1 R/\lambda)\}^{(\alpha_3)_2} \times \ldots \times \{\exp(-a_1 R/\lambda)\}^{(\alpha_3)_1}]$ (A.1.3) AS_{ABS}: Coefficient of absorptions (λ): Carrier wavelength $a_{1, 2, \ldots}$: Attenuation coefficients along segmented sections of the medium $(\alpha_3)_{1, 2, \ldots}$: Characteristic exponents on absorption effects along segmented sections of the medium Scintillation-related PLR: $[P_R / P_T]_{PL2(TS)} = [AS_{TS}\{(BW, f/f_c, D/\lambda), b(h_t/\lambda, n, \theta/\theta_o, R_e/R, D/\lambda, \eta)\}]^{(\alpha_3)_{TS}}$ (A.1.4) AS_{TS}: Coefficient of scintillation effects BW: RF passband-width (f): Carrier wavelength (in Hz)

(λ): Carrier wavelength in the medium
f_c: A cross-wind velocity factor (in per second)
b(.): An antenna averaging function
h_t: Height of the turbulent layer;
$(\alpha_3)_{TS}$ and n: Characteristic exponents
R_e: Earth's radius
(D, η): Antenna aperture diameter and illumination efficiency
(θ/θ_o): Elevational and/or azimuthal angles normalized with reference values

PL3: RF-signal power degradations due to reflection, scattering, diffractions, and/or shadowing or blocking phenomena across open-terrains/indoor premises in the LoS and/or non-LoS, multipath transits: Reflection, scattering, diffraction or shadowing specific terrain- or indoor-based EM losses.

Relevant PLRs and the associated constituent entities are as follows:

PL3-reflection:

$$[P_R/P_T]_{PL3-r} = [T\{\theta_i, \theta_r, (Z^{TM}/Z_o), (Z^{TE}/Z_o)\}]^{(\alpha_4)_r} \quad \text{(A.1.5)}$$

T: Power-transmission coefficient equal to: 1 − |Γ|, where Γ is the power-reflection coefficient
(θ_i and θ_r): Incident and reflected angles
(Z^{TE} and Z^{TM}): TE (transverse electric) and TM (transverse magnetic) wave impedances of the medium
Z_o: Free-space wave (characteristic) impedance (= 120 ×π ohm)
$(\alpha_4)_r$: Characteristic exponents for reflection-specific PLR

PL3-diffused scattering:

$$[P_R/P_T]_{PL3-ds} = [S\{(A_s/L^2), F_s(\theta_1, \theta_2, \theta_2), r_{TE/TM}(\theta_1, \theta_2, Z^{TM}/Z_o, Z^{TE}/Z_o), g\langle d\rangle/\lambda\}]^{(\alpha_4)_{ds}} \quad \text{(A.1.6)}$$

S: Scattered (power) coefficient (dependent on the type of scatterers)
A_s: Scattering rough-surface area
L: Correlation-length across surface undulations or adjacent heights
(θ_1, θ_2, θ_3): Angles defined as per Kirchhoff's scattering theory
F_s(.): Scattering-specific function
g<.>: Rayleigh's roughness factor: (A function of average surface-undulation height (d) to wavelength ratio: $\langle d\rangle/\lambda$)
$r_{TE/TM}$: Fresnel's reflection coefficient for TE/TM polarizations
$(\alpha_4)_{\delta\sigma}$: Characteristic exponents for diffusion-specific PLR

PL3-diffraction:

$$[P_R/P_T]_{PL3-D} = [D\{(R/\lambda), (\theta_i, j_d), (l^{2or3}/R^{2or3}), (y/\lambda)\}, \{(h_T/\lambda), (h_R/\lambda)\}, \{\Gamma_F, T\}, N]^{(\alpha_4)_D} \quad \text{(A.1.7)}$$

D: Diffraction coefficient
ℓ: Obstacle (linear geometry) size
y: Off-set distance in the shadow-zone
ϕ_d: Diffracted angle
(h_R and h_T): Heights of transmitting and receiving antennas
N: Number of diffracting obstacles successively located along R

T: Power-transmission coefficient equal to: $(1 - |\Gamma_\Phi|)$, where Γ_F is the power-reflection coefficient of forward reflection
$(\alpha_4)_D$: Exponent for diffraction effects

PL3-shadowing:

$$[P_R / P_T]_{PL3-sh} = [SH\{(H_B / \lambda), (\theta_i, \phi_d)\}]^{(\alpha_4)_{sh}} \quad \text{(A.1.8)}$$

SH: Shadow-caused power coefficient
H_B: Height of the shadow-casting obstacle
(θ_i and ϕ_d): Incident and diffracted angles
$(\alpha_4)_D$: Exponent for shadowing effects

PL4: Fading (frequency/time/spatial) specific RF power-losses – Fading (Frequency/time/spatial) associated RF power-losses in outdoor and indoor settings:

$$[P_R / P_T]_{PL4} = [FD\{(R / \lambda), (C / \lambda^2)\}, \{(h_T / \lambda), (h_R / \lambda), \}, f_c\{G / \lambda, n\}, \{(v / v_o), (u / u_o)\}]^{(\alpha 5)_{FD}} \quad \text{(A.1.9)}$$

FD: Fading-specific power-loss coefficient
C: Cell-size (area)
G: An index for the geometrical disposition of the contents/obstacles
(h_R and h_T): Heights of transmitting and receiving antennas
(v and u): Velocities of mobile user and moving obstacles (like foliage movement due to wind) respectively referenced with respect to: $\{v_o, u_o\}$
$(\alpha_5)_{FD}$: Exponent for fading effects

PL5: RF-power loss *versus* depolarization (intentional and/or unintentional) effects) - EM wave depolarization effects

$$[P_R / P_T]_{PL5} = [PO\{(R / \lambda), (IRA / \lambda^2), n_{IR}\}, \{(\theta_T / \theta_R), (\varphi_T / \varphi_R)\}]^{(\alpha_6)_{PO}} \quad \text{(A.1.10)}$$

PO: Polarization-specific power-loss coefficient
IRA: Irregular geometry area causing depolarization
n_{IR}: Number of depolarizers
(θ_T and θ_R): Angular dispositions of transmitting and receiving antennas relative to (ϕ_T and ϕ_P) depicting azimuthal angular dispositions of transmitting and receiving antennas
$(\alpha_6)_{PO}$: Exponent for polarization effects

PL6: Transceiver mobility-specific path-loss attributes due to Doppler spread (Doppler-shift in carrier frequency)

$$[P_R / P_T]_{PL6} = [DD\{(x / x_o, y / y_o)_T, (x / x_o, y / y_o)_R, (v_A / v_o)_T, (u_A / u_o)_R, (\pm \Delta f / f), n_{mp}\}]^{(\alpha 7)_{Dop}} \quad \text{(A.1.11)}$$

DD: Doppler-shift specific power-loss coefficient
$(x, y)_{T, R}$: Coordinates of the transmitter T and receiver R relative to (x_o, y_o) at any instant of observation
(v_A and u_A): Velocities of transmitting and receiving antennas relative to (v_o and u_o)
Δf: Doppler-shift

PL7: Transceiver site-specific power-delay profile *versus* path-loss characteristics: RF power-delay *versus* path-loss characteristics:

$$[P_R/P_T]_{PL7} = [DE\{(R_i/\lambda)_{i=1,2,...M}, (\tau_{rms}/\tau_o), <(\tau/\tau_o)>\big|_{spatialaverage}, <(W(R_i\tau/\lambda\tau_o)/W_o)>\big|_{spatialaverage}, C(f)/C_{peak}, (h_T/\lambda, h_R/\lambda)\}]^{(\alpha_8)_{pdl}} \quad \text{(A.1.12)}$$

DE: Delay-specific power-loss coefficient; (i = 1, 2, …, M); M denotes the index for M-multipaths

(τ_{rms}/τ_o): RMS delay-time referenced to τ_o

$<(\tau/\tau_o)>$: Spatial average over the service area

$<(W/W_o)>$: Spatial average of total energy (in normalized form) integrated over average time-delay

$C(f)/C_{peak}$ Coherence function relative to its peak value

$(\alpha_8)_{pdl}$: Exponent for delay effects

PL8**:** Power-loss due to antenna beam-shape or lobing, collapsing losses (caused by diversity etc.), RF system-specific filter losses and defocusing effect

PL8-(A): Antenna beam shape/lobes

$$[P_R/P_T]_{PLS-(A)} = [CL_{absl}(\exp\{k_\theta\theta_i^2/\theta_{3dB}^2 + k_\phi\phi_i^2/\theta_{3dB}^2\})_{i=1,2,...M}/(P_{MB})]^{(\alpha_9)_{abl}} \quad \text{(A.1.13)}$$

CL_{absl}: Antenna-beam shape/lobes specific power-loss coefficient

(θ_i and ϕ_i): Angular separation between transmitter and receiver in elevational and azimuthal planes

(k_θ, k_ϕ): Corresponding (Gaussian) beam-shaping constants referenced to 3-dB beam-widths, (θ_{3dB} and ϕ_{3dB})

P_{MB}: Main-lobe (LoS) transceive power

$(\alpha_9)_{abl}$: Exponent for antenna beam-shape effects

PL8-(B): Collapsing loss

$$[P_R/P_T]_{PLS-(B)} = [CL_{cl}(SNR)_D/SNR]^{(\alpha_9)_{cl}} \quad \text{(A.1.14)}$$

CL_{cl}: Collapsing-loss coefficient (at the output $(SNR)_D$ when diversity (D) is deployed with additional noise contribution

SNR: Output SNR with no diversity; $(\alpha_9)_{cl}$: Exponent for collapsing-loss effects

PL8-(C): Filter loss - RF-system (hardware) specific losses and co- and adjacent-channel interference specific signal artifacts/power-losses.

$$[P_R/P_T]_{PLS-(C)} = [CL_{fl}(TF)_{actual}/(TF)_{ideal}]^{(\alpha_9)_n} \quad \text{(A.1.15)}$$

CL_{fl}: Filter-loss due to transfer function integrity of the actual processor (filter) *versus* transfer function integrity of an ideal processor (filter) in the system

$(\alpha_9)_{fl}$: Exponent for filter-loss effects

PL8-(D): Defocusing loss:

$$[P_R/P_T]_{PLS-(D)} = [CL_{df}\{(m_{r-h})_{actual}/(m_{r-h})_{reference}, \theta_e/\theta_{e-reference}\}]^{(\alpha_9)_{df}} \quad \text{(A.1.16)}$$

CL_{df}: Defocusing-loss due to atmospheric/climatic effects with variations of refractive index (m_r) as a function of the height, h

θ_e: Elevation angle of the transit-path of RF energy

$(\alpha_9)_{df}$: Exponent for filter-loss effects

References

[1]. Torkildson, E., Zhang, H., Madhow, U. *Channel modeling for millimeter wave MIMO*. Information Theory and Application Workshop on; 2010, paper_155

[2]. Ghosh, A. *The 5G mmWave radio revolution*. Microwave Journal, 2016, 59(9): p. 22-36.

[3]. Buckingham, E. *Model experiments and the form of empirical equations*, Transactions ASME, 1915, 37: p. 263-296.

[4]. Neelakanta, P. S., Chatterjee, R., *Antennas for Information Super Skyways- An Exposition on Outdoor and Indoor Wireless Antennas*, 2003, Research Studies Press, England, UK.

[5]. Lee, W. C. Y., *Mobile Cellular Telecommunications*, McGraw-Hill, Inc, 1995, New York, NY, USA.

[6]. Bertoni, H. L, *Radio Propagation for Modern Wireless Systems,* Prentice-Hall, 2000, Upper Saddle River, NJ, USA.

[7]. Parsons, D., *The Mobile Radio Propagation Channel*, John Wiley & Sons, 1992, New York, NY, USA.

[8]. Jakes, W. C. (Ed.), *Microwave Mobile Communications*, IEEE Press, 1974, Piscataway, NJ, USA.

[9]. Yu, K., Ottersten, B., *Models for MIMO propagation channels: a review*. Wireless *Communications and Mobile Computing*, 2002, 2: p. 653-666.

[10]. Zheng, K., Ou, S., Yin, X., *Massive MIMO channel models: A survey*. International Journal of Antennas and Propagation, 2014, 2014: p. 1-10.

[11]. Özcelik, H., Czink, N., Bonek, E., *What makes a good MIMO channel model*? Proceedings of 2005 IEEE 61st Vehicular Technology Conference (VTC 2005-Spring, May 30 June 1, 2005, Stockholm, Sweden): p. 156-160.

[12]. Telatar, I. E., *Capacity of multi-antenna Gaussian channels*. European Transactions on Télécommunications, 1999, 10(6) : P. 585-595.

[13]. Foschini, G. J., Gans, M. J., *On limits of wireless communications in a fading environment*. Wireless Personal Communications, 1998, 6: p. 311-335.

[14]. Pi, Z., Khan, F., *An introduction to millimeter-wave mobile broadband systems*. IEEE Communications Magazine, June 2010: p. 101-107.

[15]. Wolowicz, C. H., J. S. Bowman, Jr., Gilbert, W. P., *Similitude requirements and scaling relationships as applied to model testing*, NASA Technical Paper, 1435, August 1979: p. 1-61.

[16]. Neelakanta, P. S., Thengum-Pallil, G. A., *Eco-friendly testing of solar cells used in ionizing radiation ambient*. Power Electronics Technology, September 2011: p. 17-19.

[17]. Liu, H., M. M., Yahia, M. Antar, Z. Shi, Wu, Z., *Application of millimeter wave in verification of scale model measurement for radar cross section*. International Journal of Infrared and Millimeter Waves, 1998, 19(4): p. 641-649.

[18]. Kline, S. J. *Similitude and Approximation Theory*, Springer Verlag, New York, NY, USA, 1986.

[19]. Heller, V. Scale effects in physical hydraulic engineering models. *Journal of Hydraulic Research*, 2011, vol. 49(3), 293-306.

[20]. Langhaar, H. L. *Dimensional Analysis and Theory of Models*, John Wiley & Sons, 1951, New York, NY, USA.

[21]. Sabnis, G. M., Harris, H. G., White, R. N., Mirza, M. S., *Structural Modeling and Experimental Techniques*. Prentice-Hall Inc., 1983, Englewood Cliffs, NJ, USA.

[22]. Schumacher, C. R., Taylor, D. W., *Electrodynamic similitude and physical scale modeling of nondispersive targets*. Journal of Applied Physics, 1987, 62(70): P.2616-2625.

[23]. Wu, Z., Liu, R., *Electrodynamic similitude and inconsistency of laser scattering for scale model.* International Journal of Infrared and Millimeter Waves. 1995, 16(7): p. 1249-1259.

[24]. Neelakanta, P. S. *Handbook of Electromagnetic Materials – Monolithic and Composite Versions and Their Applications*, CRC Press, 1995, Boca Raton, FL, USA.

[25]. Burton, R. W., King, R. W. P., Wu, T. T., *The loop-antenna and cylindrical core: theory and experiment*. IEEE Transactions on Antennas and Propagation, 1983, 31(3): p. 225-231.

[26]. Lemorton, J., Castanet, L., Lacoste, F., van de Kamp, M., *Development of propagation models for telecommunication satellite systems*. *Final Report*, July 2004– ESA/ESTEC/Contract No. 16865/03/NL/EC.

[27]. ITU-R: *Propagation data and prediction methods required for the design of Earth-space telecommunication systems*. Question ITU-R 206/3 - RECOMMENDATION ITU-R P.618-7, Geneva.

[28]. Panagopoulos, A. D., Kanellopoulos, J. D., *Statistics of differential rain attenuation on converging terrestrial propagation paths*. IEEE Transactions on Antennas and Propagation, 2003, 51(9): p. 2514–2517.

[29]. Neelakanta, P. S., De Groff, D., R. Sudhakar, R. *Low-altitude target detection by coastline operated marine radar.* IEEE Transactions on Aerospace and Electronic Systems, 1992, AES 28(1): p. 217-222.

[30]. Aalo, V., J. Zhang, J., *Effect of macrodiversity on average-error probabilities in a Rician fading channel with correlated lognormal shadowing*. IEEE Transactions on Communications, 2001, 49(1): p. 14-18.

[31]. Aalo, V., Zhang, J., *Performance analysis of maximal ratio combining in the presence of multiple equal-power co-channel interferers in a Nakagami fading channel*. IEEE Transactions on Vehicular Technology, 2001, 50 (2): p.497-503.

[32]. Aalo, V., Piboongungon, T., Iskander, C. D., *Bit-error rate of binary digital modulation schemes in generalized gamma fading channels,* IEEE Communications Letters, 2005,.9(2): p.139-14.

[33]. Aalo, V., Ermolova, N. Y., Efthymoglou, G. P., *Channel capacity and average error rates in generalized-K fading channels*. IEEE Transactions on Communications, 2010, 4(11): p. 1364-1372.

[34]. Piboongungon, T., Aalo, V., *Outage probability of L-branch selection combining in correlated lognormal fading channel,* Electronics Letters, 2004, 40(14): p. 886-888.

[35]. Chayawan, C., Aalo, V., *On the performance of optimum combining and maximal ratio combining schemes in a Rice fading channel with co-channel interference*, IEEE Transactions on Communications*,* 2002*,* 50(4): p. 532-535.

[36]. Zhang, J., Aalo, V., *Effect of macrodiversity on average error probabilities in a Rician fading channel with correlated lognormal shadowing,* IEEE Transactions on Communications*,* 2001, 49(1): p.14-18.

[37]. Efthymoglou, G., Aalo, V., *Path diversity performance of a DS-CDMA based Land-mobile satellite system in a shadowed Rician fading channel with power control error*. IEEE Transactions on Vehicular Technology, 2000, 49(6): p. 2051-2059.

[38]. Efthymoglou, G., Aalo, V., *Path diversity performance of a DS-CDMA based Land-mobile satellite system in a shadowed Rician fading channel with power control error*. IEEE Transactions on Vehicular Technology, 2000, 49(6): p. 2051-2059.

[39]. Anastasov, J. A., Djordjevic, G. T., Stefanovic, M. C., *Analytical model for outage probability of interference-limited systems over extended generalized-K fading channels*. IEEE Communications Letters, 2012, 16(4): p. 473-475.

[40]. Dogandžic, A., Jin, J., *Estimating statistical properties of MIMO fading channels*. IEEE Transactions on Signal Processing, 2005, 53(8): p. 3065-3080.

[41]. Rice, P. L. Longley, A. G., Norton, K.A., Barsis, A. P., *Transmission loss predictions for tropospheric communication circuits*. NBS Technical Note 101, 1965/1966, 2: p.1.1-12.10.

[42]. Okumura, Y., Ohmori, T, Kawano, T., Fakuda, K., *Field strength and its variability in VHF and UHF mobile radio service*. Review on Electrical Communication Laboratory, 1968, 16(9-10): p. 825-873.

[43]. Hata, M., *Empirical formula for propagation loss in land mobile radio services.* IEEE Transactions on Vehicle Technologies, 1980, VT-29(3): p. 317-325.

[44]. Walfish, J., Bertoni, H. L., *A theoretical model of UHF propagation in urban environments*. IEEE Transactions on Antennas and Propagation, 1988, AP-36(1): p. 1788-1796.

[45]. Turin, G. I., Clapp, F. D., Johnston, T. L., Fine. S. B., Lavry, D., *A statistical model of urban multipath propagation.* IEEE Transactions on Vehicle Technology, 1972, VT-21(1): p. 1-9.

[46]. Hashemi, H., *Indoor radio propagation channel*. IEE Proceedings, 1993, 81(7): p. 941-968.

[47]. Molkdar, D., *Review on radio propagation into and within buildings*. Proceedings of the IEEE, 1991, 138(1): p. 61-73.

[48]. Rappaport, T. S., Seidel S. Y., Takamizawa, K., *Statistical channel impulse response models for factory and open plan building radio communication design.* IEEE Transactions on Communications, 1991, COM-39(5): p. 794-806.

[49]. Saleh, A. M., Valenzula, R. A., *A statistical model for indoor multipath propagation*. IEEE Journal on Selected Areas in Communications, 1987, SAC-5(2): p. 126-137.

[50]. Seidel, S. Y., Rappaport, T. S., *914 MHz path-loss prediction models for indoor wireless communications in multifloored buildings.* IEEE Transactions on Antennas and Propagation, 1992, AP-40(2): p. 1-11.

[51]. Neelakanta, P. S., Dighe, H., *Robust factory wireless communications*: *A performance appraisal of the Bluetooth ™ and ZigBee™ collocated in an industrial floor*. Proceedings of the 29th Annual Conference of the IEEE Industrial Electronics Society (IECON 2003), (November 2-6, 2003, Roanoke, Va USA): p.2371-2376.

[52]. Y. Wang, Lu, W., Zu, H., *An empirical path-loss model for wireless channels in indoor short-range office environment*, International Journal of Antennas and Propagation, 2012, 2012: p. 1-7.

[53]. Crane, R., *ACTS propagation experiment: Experiment design, calibration, and data preparation and archival*. 1997, Proceedings of the IEEE, 85: p. 863-878.

[54]. Crane, R., *Electromagnetic Wave Propagation through Rain*, John Wiley and Sons, 1996, New York, NY, USA.

[55]. Slobin, S. D., *Atmospheric and environmental effects:* In: DSN Telecommunications Link Design Handbook, 2009. DSN No. 810-005, Space Link Interfaces, Module 105, Rev. D, Jet Propulsion Laboratory, Pasadena, California, September 15, 2009.

[56]. ITU-R: *Attenuation by atmospheric gases*. Question ITU-R 201/3 - RECOMMENDATION ITU-R P.676-3(1990-1997), Geneva.

[57]. ITU-R: *Attenuation in vegetation*. Question ITU-R 202/3 - RECOMMENDATION ITU-R P.833-2 (1992-1999), Geneva.

[58]. Caesar, J. R. Bello, D. Siqueira, G. L., Bertoni, H. L., *Theoretical analysis and measurement results of vegetation effects on path loss for mobile cellular communication systems*. IEEE Transactions on Vehicular Technology, 2000, 49(4): p. 1285-1293.

[59]. Xu, Z., Dong, X., Bornemann, J., *Design of a reconfigurable MIMO systems for THz communications based on grapheme antennas*. IEEE Transactions on Terahertz Science and Technology, 2014, 4(5): p. 609-617.

[60]. Song, H., Nagatsuma, T., *Present and future of terahertz communications*, IEEE Transactions on Terahertz Science and Technology, 2011, 1(1): p. 256-263.

[61]. Koch, M. *Terahertz communications : A 2020 vision*. In R. E. Miles et al. (Eds.), Terahertz Frequency Detection and Identification of Materials and Objects, Spring Verlag, 2007, Berlin, Germany, p.325-338.